The Price of Weather:

Unspanned ENSO Risk in Commodity Futures

Zong-Wei Yeh* Dongjie Fang†

October 2, 2026

Abstract

The El Niño–Southern Oscillation (ENSO) is declared by a public agency months before its economic effects arrive, and is almost invisible in commodity futures curves, yet it forecasts the returns those curves deliver. In nine commodities over 1990–2026, a 1°C higher Oceanic Niño Index lowers expected one-month excess returns on the six weather-sensitive commodities by about 16% per year, while the three metals, whose supply does not run through growing or heating conditions, show none. The predictability is concentrated in the cold season, at horizons of a few months, and in La Niña states; commercial hedgers shift their positions in the same states. A no-arbitrage model in which ENSO shifts the distribution of future prices without entering the pricing equation implies a premium that declines with maturity, a profile that the reduced-form evidence does not impose and the data do not reject. Weather is priced in commodity futures, not in the curve but in the returns.

Keywords: commodity futures, ENSO, unspanned macro risk, affine term structure model, hedging pressure, theory of storage.
JEL codes: G12, G13, Q02, Q54.

*Department of Money and Banking, National Chengchi University. Email: 111352502@nccu.edu.tw.
†Kate Tiedemann School of Business and Finance, University of South Florida. Email: dfang@usf.edu.

1 Introduction

The state of the El Niño–Southern Oscillation (ENSO) is public months before the weather it brings. NOAA publishes the index that measures it on a fixed monthly schedule, and the index leads the regional weather it organizes by a season (Iizumi et al., 2014; Cashin et al., 2017).[1] Yet the ENSO state is almost absent from commodity futures curves. This paper shows that it forecasts the excess returns on futures for the commodities whose supply or demand runs through the weather, and that it does not forecast the returns on metals. We interpret the result through the theory of storage, in which the premium earned by long positions depends on how scarce the commodity is. The paper establishes the predictability, develops a no-arbitrage model in which ENSO moves expected returns without entering prices, and presents evidence from the timing of the effect, the futures basis and the positions of commercial hedgers that supports the storage interpretation.

Whether a public climate state forecasts returns is a question on which two views of a futures market disagree. If the curve summarizes what the market knows, a state that is announced months ahead should already be in prices, and conditional on the curve it should say nothing about returns. If premia vary with the state of inventories, as the theory of storage holds, a state that shifts expected supply also shifts the premium, and it can do so without moving the price. Evidence that macroeconomic information forecasts returns beyond the curve exists for bonds and for oil (Joslin et al., 2014; Heath, 2019). The macroeconomic variables usually proposed as unspanned risks are endogenous to the markets they help explain, measured with delay and revised after publication, which makes the two views hard to separate.

ENSO has none of these features. We measure it with the Oceanic Niño Index, an index of equatorial Pacific sea-surface temperature published by NOAA's Climate Prediction

[1] On 8 June 2023 the Climate Prediction Center raised its ENSO alert status to an El Niño Advisory, months before the winter in which the associated heating- and growing-season effects were realized (*ENSO Diagnostic Discussion*, 8 June 2023). The Center publishes a diagnostic discussion each month, sets an alert status of Watch, Advisory or Final Advisory, and releases the Oceanic Niño Index used in this paper on the same schedule.

Center. The index is generated by an ocean–atmosphere oscillation that no economic decision affects. It is a single state, published on a fixed schedule and never the outcome of trading. And it matters for the economy through specific physical channels, growing conditions and heating demand, so that commodities outside those channels can serve as a placebo. Temperature and rainfall, the variables with which the physical literature begins, are local realizations, and over a long sample they are not exogenous to economic activity. The cost of this choice is that ENSO is only one source of weather variation.

We study nine commodities at the monthly frequency from 1990 to early 2026: corn, soybeans and wheat; crude oil, heating oil and natural gas; copper, gold and silver. We call the first six weather-sensitive, because their supply or demand runs through growing conditions or heating demand. The three metals are stored, financialized and traded on the same exchanges by the same investors, but they are not exposed to the channel we study. Two principal components describe each commodity's futures curve almost perfectly, and in every one of the nine markets they span only a small fraction of the variation in the ENSO index. We then regress one-month excess returns on the ENSO state, controlling for the two curve factors. A 1°C higher index lowers the expected excess return on the weather-sensitive commodities by about 16% per year. The slope is negative for each of the six, it is largest and most stable over time for crude oil and heating oil, and it is indistinguishable from zero for the metals. The sign is the one the storage interpretation predicts: a higher index means El Niño, abundance and a smaller premium for holding the commodity, and La Niña means scarcity and a larger one. The effect is large for a return forecast and modest next to the volatility of commodity returns. Inference by block bootstrap, which preserves the persistence of the index, leaves these results in place.

The interpretation starts from an identity: a futures price is the expected future spot price net of the premium that long positions earn. Suppose El Niño signals greater expected supply. The expected spot price falls, which pushes the futures price down. More abundant inventories also reduce the compensation that inventory-holding intermediaries and long

futures investors require, which pushes the futures price up. The two effects offset in the price, and the premium appears in subsequent returns, so ENSO can matter economically while leaving only a weak imprint on the contemporaneous curve. It is a hidden factor in the sense of Duffee (2011). The same economics gives the response its shape. Premia and convenience yields fall as inventories rise, and they fall convexly, because near a stockout an extra unit of expected supply moves the marginal value of storage a great deal while in times of plenty it moves it hardly at all (Deaton and Laroque, 1992; Gorton et al., 2013). La Niña pushes these commodities toward the steep part of that relation and El Niño toward the flat part.

Five further findings support the storage interpretation. First, the predictability is concentrated in the boreal cold season, when the Pacific teleconnection over the Americas is strongest and the northern heating season and the South American growing season coincide. Second, for the weather-sensitive commodities as a group it is strongest at horizons of one to three months and gone by a year, the profile of a transitory shock to a storable good. Third, the response comes from La Niña states: crude oil earns a large positive return in La Niña months and a negative one in El Niño months. Fourth, a higher index tilts the curves of the weather-sensitive commodities toward contango in the same month, as a move toward abundance should, and it does not move the curves of the metals. Finally, in CFTC positioning data, commercial hedgers are more net short in La Niña than in El Niño for each of the six weather-sensitive commodities, while the metals as a group show no such difference. Producers hedge more heavily in La Niña, the state in which realized returns are highest. Adding hedging pressure and the speculative net position to the return regression leaves the ENSO slopes of the energy commodities and corn essentially unchanged. The two are complements: ENSO shifts the quantity of risk to be borne, and positions record who bears it.

A no-arbitrage model ties the evidence together. In the model, futures prices are set by the two curve factors alone, and ENSO enters the dynamics that govern how those

factors evolve. The model is fitted to the level of the premium, so its content lies in the profile of the premium across maturities. It implies a premium that declines as contracts lengthen, at a rate governed by how quickly the market prices the underlying shocks as mean-reverting; the persistence of ENSO plays no part in it. The reduced-form evidence does not impose that shape. When we estimate the ENSO slope freely at five points along the curve and test those estimates against the model's profile, the profile is not rejected for any of the nine commodities. The premium decays with maturity as a Samuelson (1965) effect predicts.

The results matter for how the curve is used. A hedging or risk-management model calibrated only to the dynamics of the curve treats the curve as a sufficient statistic for future prices and returns. For the weather-sensitive commodities that premise fails in a forecastable way: the ENSO state is known, it is not in the curve, and it shifts expected returns for several months. The results also bear on where to look for physical climate risk. A climate state can matter for a market without being visible in its prices.

Related literature and contribution. This paper builds on the literature on commodity risk premia and the theory of storage. Fama and French (1987), Bessembinder (1992), Gorton et al. (2013) and Szymanowska et al. (2014) establish that premia and convenience yields decrease in inventories, that the relation is convex because the stockout constraint binds in scarcity (Deaton and Laroque, 1992), and that commercial hedging demand is compensated. The recurring difficulty is that inventories, hedging demand and prices are determined jointly, so a regression of the premium on the inventory state is hard to interpret. We add a state variable that is exogenous to these markets and whose sign is fixed in advance by atmospheric physics. It lets us read the convexity of the storage relation off the ENSO phase instead of off an endogenous inventory measure, and observe hedging pressure responding to the same state that moves the premium.

Our work also adds to the literature on unspanned risk in term-structure models. Joslin

et al. (2014) and Duffee (2011) show that macroeconomic information can move bond risk premia while remaining nearly orthogonal to the yield curve, within the affine framework of Ang and Piazzesi (2003) and Joslin et al. (2011). In commodities, Heath (2019) finds unspanned real-activity and inventory information in oil futures, and Jacobs et al. (2017), in the electricity market, develop the two-step spanning test we use. What this literature has lacked is a state variable whose unspannedness can be argued from outside the data. ENSO is exogenous, published on a fixed schedule and observed for nine markets at once, so the same spanning test can be run across a cross-section that includes markets in which the mechanism should be absent. We also give a reason for the unspannedness, the offsetting of the expected spot price and the premium.

Finally, the paper relates to the empirical work on ENSO and on physical climate risk. A body of work documents the effects of ENSO on commodity prices, crop yields and macroeconomic aggregates.[2] This work concerns prices. We ask whether ENSO is compensated in subsequent expected returns, which requires separating expectations from premia and can give an answer of the opposite sign. What we study is interannual climate variability, a different object from climate change. The climate finance literature surveyed by Giglio et al. (2021) has concentrated on long-horizon risks (Barnett et al., 2020; Baldauf et al., 2020). We examine a short-horizon physical channel that is visible at a monthly frequency in a liquid, centrally cleared market, and its link to climate change runs through the projected frequency of extreme events (Cai et al., 2014).

The rest of the paper is organized as follows. Section 2 describes the data and the spanning evidence. Section 3 presents the return predictability. Section 4 develops and estimates the no-arbitrage model. Section 5 provides further evidence on the storage interpretation. Section 6 concludes. Tables and figures follow the references, and Appendices A to C contain the derivation, the estimation details and additional tables.

[2] Brunner (2002), Cashin et al. (2017) and Ubilava (2018) document effects of ENSO on commodity prices and macroeconomic aggregates, Iizumi et al. (2014) quantify the crop-yield channel, and Ubilava (2017) finds asymmetry in wheat prices on the El Niño side.

2 Data and the Spanning of ENSO

This section describes the futures data and the construction of returns, the ENSO state and its timing, the data on positions and physical quantities, and the extent to which the futures curve spans ENSO.

2.1 Contracts, calendars and returns

We use month-end exchange settlement prices of generic n-th nearby futures contracts for nine commodities from LSEG, at seven points on the curve, $n \in \{1, 2, 3, 4, 5, 6, 8\}$.[3] The three sectors are agriculture (corn, soybeans, wheat), energy (WTI crude oil, heating oil, natural gas) and metals (copper, gold, silver), and we refer to the first two together as weather-sensitive. Three ICE softs, cotton, coffee and sugar, are used in an extension reported in Section 3. The baseline return is the return on the second nearby contract. The front contract is affected by trading in the expiry week and, under a seasonal listing calendar, its months to expiry vary irregularly.

A generic n-th nearby is a contract, which is not the same thing as a maturity. The three NYMEX energy chains and COMEX copper list every calendar month, so for them the n-th nearby has n months to expiry. CBOT grains trade seasonal cycles with no serial months (corn and wheat March, May, July, September, December; soybeans January, March, May, July, August, September, November), and COMEX gold and silver trade a cycle plus the three nearest calendar months. We compute months to expiry $\tau_{t,n}$ from the delivery cycle of each exchange and validate it against the exchange expiry date carried in the settlement file. The two agree, allowing a constant offset, for 93.8% to 100% of contract-months.[4]

[3] The seventh nearby is thin, and the tenth and twelfth nearby begin too late for several commodities. Settlement is the price at which the exchange marks positions, and the settlement panel is more complete than the last-trade field, which is missing where contracts are thin. Appendix Table A10 compares the two.

[4] A constant offset reflects the convention of quoting the delivery month instead of the expiry month; it is one month for heating oil, whose contracts expire in the month before delivery. The offset cancels in the basis denominator and is absorbed by the pricing intercepts. Appendix Table A11 reports roll and liquidity diagnostics.

Months to expiry enter in three places. First, excess returns follow the contract through the roll. The return on the n-th nearby contract is

$$rx_{t+1}^{(n)} = f_{t+1}^{(j(t,n))} - f_t^{(n)}, \tag{1}$$

where $f_t^{(n)}$ is the log price at t of the n-th nearby and $j(t,n)$ is the generic whose months to expiry at $t+1$ equal $\tau_{t,n} - 1$, that is, the generic that holds at $t+1$ the same contract that was the n-th nearby at t. Where $\tau_{t,n} = n$ this is the familiar roll from the n-th to the $(n-1)$-th nearby; for the grains it alternates, and for gold and silver the position stays on the same generic for several months. Second, the basis is annualized by the actual expiry gap, $(f_t^{(1)} - f_t^{(6)})/(\tau_{t,6} - \tau_{t,1}) \times 1200$, with a positive value meaning backwardation. That gap is five months for the energy chains and copper and averages 12.0 months for corn and wheat, 8.4 for soybeans and 7.5 for gold and silver. Third, the measurement equation of the affine model in Section 4 prices contract (t,n) at maturity $\tau_{t,n}$.

Every panel is placed on a complete monthly grid before any lead, lag or difference is taken, so that a one-month operation spans exactly one calendar month. Seven of the nine commodities have no missing months. Wheat has the most, with 57 months missing and a longest gap of 42 months.

2.2 The ENSO state and its timing

The ENSO state is measured by the Oceanic Niño Index (ONI), the three-month running mean of sea-surface temperature anomalies in the Niño 3.4 region published by NOAA's Climate Prediction Center. Positive values are El Niño conditions and negative values La Niña; Figure 1 plots the series with the phases shaded. ENSO is exogenous to trading activity, so reverse causality is not a concern (Cashin et al., 2017), and it leads regional weather anomalies by three to six months (Iizumi et al., 2014). A single index also avoids the multiple-testing problem of commodity-by-commodity weather variables (Ubilava,

2018).

The ONI stamped at month m is centered on m and published early in month $m+2$. Our state is therefore

$$M_t = \text{ONI centered at month } t-2, \tag{2}$$

which is published early in month t and is in the end-of-month-t information set.[5]

The state has a standard deviation of 0.843°C, ranges from -1.66 to $+2.75$, and has a monthly autocorrelation of 0.973, so the sample contains about a dozen independent episodes.[6] We report two kinds of inference. Asymptotic standard errors are those of Newey and West (1987) with 12 lags for single-commodity regressions, or $\max(12, h+1)$ lags at horizon h, and those of Driscoll and Kraay (1998) with Bartlett weights and 12 lags for panels. For the main estimates we add p-values from a circular moving-block bootstrap over months with 24-month blocks, which resamples whole cross-sections and so preserves both the persistence of M_t and the dependence across commodities. The asymptotic errors do not depend on a resampling scheme, and the bootstrap accounts for the small number of episodes.

2.3 Positions and physical quantities

Section 5 uses three further sets of data. The first is the CFTC's legacy futures-only Commitments of Traders reports, from which we compute hedging pressure, $HP_t = (\text{commercial short} - \text{commercial long})/\text{open interest}$, and the speculative net position. We take the last report of each month and stamp it by its release month. A legacy report is dated as of a Tuesday and published the following Friday, which falls in the next calendar

[5] The curve factors and the portfolio controls are extracted with full-sample principal-component moments, as is standard in this literature, and the heating-degree-day anomaly described below is deseasonalized with full-sample calendar-month means. The ENSO state is the only conditioning variable constructed in real time.

[6] The persistence of a predictor is the source of the bias in Stambaugh (1999), which is proportional to the correlation between the innovation to the predictor and the innovation to the return. ENSO innovations are ocean–atmosphere shocks that cannot respond to commodity market outcomes, so that correlation is essentially zero.

month for 43.5% of commodity-months, so an as-of stamp would put HP_t outside the end-of-month-t information set.[7] The compressed CFTC history begins in 1995 for energy and metals and in 1998 for the three CBOT grains, and regressions that use positions are estimated on that window.

The second is the contiguous-U.S. heating-degree-day series of NOAA's National Centers for Environmental Information, from which we form an anomaly by removing calendar-month means. The third is the Energy Information Administration's series of distillate stocks and natural gas storage, each lagged by its publication delay. The futures basis defined above completes the set: it is observed for all nine commodities and, unlike inventories, is available without delay.

2.4 Curve factors and spanning

For each commodity we extract two principal components from the demeaned matrix of log futures prices, signing them so that a higher PC^1 means higher prices and a higher PC^2 means backwardation (Appendix Figure A1). Table 1 reports the samples, the variance decomposition and the projection of M_t on $L_t = (PC^1_t, PC^2_t)'$. Two factors capture at least 99.1% of the cross-sectional variation in every commodity, the familiar level and slope structure. The same two factors span little of ENSO: the R^2 of the projection is 0.085 for crude oil and lower for the other eight commodities. For crude oil and heating oil the larger part of what the curve spans is on the slope factor, and for the other commodities it is on the level factor (Appendix Table A3, Panel A).

The projection R^2 shows that little of ENSO is in the curve. Whether the part outside the curve matters for prices is a separate question, which the second step of the Jacobs et al. (2017) test addresses. The residual of the projection predicts next month's change in

[7] Reports are matched on the CFTC contract market code, because market names change over the sample: corn 002602, soybeans 005602, SRW wheat 001602, WTI crude 067651, NY Harbor ULSD 022651, Henry Hub natural gas 023651, copper 085692, gold 088691, silver 084691. Stamping by the as-of date changes the pooled gap reported in Section 5 from 0.052 to 0.054.

the level factor for corn, crude oil and heating oil, at the 1% level in each case (Appendix Table A3). The sign is negative: a higher ENSO state today is followed by a lower level of the curve next month, beyond what the curve itself predicts. If ENSO forecasts returns, it does so through the physical dynamics of the curve factors, since it is nearly absent from the cross-sectional pricing equation. The next section examines returns directly.

3 ENSO and Expected Returns

This section shows that the ENSO state forecasts excess returns on the weather-sensitive commodities and not on the metals, and that the predictability is concentrated in the cold season, at short horizons and in La Niña states.

3.1 Main results

Our baseline regression is

$$rx_{t+1}^{(n)} = \alpha + \boldsymbol{\beta}_{pc}' L_t + \beta_M M_t + \varepsilon_{t+1}, \tag{3}$$

where $rx^{(n)}$ is the excess return of equation (1). Returns, premia and slopes are expressed in percent per year throughout the paper, with monthly log returns multiplied by 1,200, so β_M is the change in the expected annualized return per 1°C of ONI, conditional on the current curve.

Table 2 reports the estimates for the second, third and sixth nearby contracts, and Figure 2 plots the second-nearby slopes. The slope is negative for every weather-sensitive commodity and significant for crude oil, heating oil and corn. It is largest for the two petroleum contracts: a 1°C higher index lowers the expected return on crude oil by 23.9% per year with a t-statistic of -3.37, and the heating oil estimate is slightly larger. The corn slope is about half that size and is also significant at the 1% level. None of the three metals

has a significant slope, and the estimates for gold and silver are positive. The pattern is the same on the third and sixth nearby contracts.

Precision, more than the size of the point estimates, separates the six weather-sensitive commodities. Natural gas has a larger point estimate than corn and the most volatile returns in the sample, so its standard error is 1.6 times that of crude oil and its slope is not individually significant. Soybeans and wheat have slopes about half the size of corn's. The uniform sign across the six, set against two positive slopes among the three metals, is what the pooled tests below exploit.

The effect is economically large. A one-standard-deviation increase in the ENSO state lowers the expected crude oil return by 20.1% per year, about one-sixth of the standard deviation of the monthly return in the same units. For the weather-sensitive commodities as a group the effect is somewhat smaller, in line with the panel slope reported below. The incremental R^2 from adding the ENSO state to the curve factors is at most 3.2%, which is in the range usual for monthly return forecasts.

The predictability is confined to commodities with physical weather exposure. In the panel of Table 3, Panel B, which stacks the nine commodities with commodity fixed effects and commodity-specific slopes on the curve factors, the ENSO slope for the weather-sensitive commodities is -15.8% per year with a t-statistic of -3.72, and the slope for the metals is close to zero. The difference between the two groups is significant at the 1% level. The equal-weighted sector portfolios of Panel A give the same ordering: energy has the largest slope, agriculture a smaller one, and metals none.[8]

The contrast holds in a tradable portfolio. A position that is long the six weather-sensitive commodities and short the three metals has an ENSO slope of -14.0% per year,

[8]Appendix Table A5 collects the robustness checks. A block bootstrap over months leaves the panel slope, the difference from metals and the crude oil, heating oil and corn slopes significant at the 5% level. An episode-level test in the spirit of Ibragimov and Müller (2010), which treats contiguous blocks of the sample as independent observations, rejects for the weather-sensitive panel slope at the 5% level with twelve blocks and at the 10% level with eight, and does not reject for the difference from metals. The estimates for energy and corn are insensitive to dating the ONI at lags of zero or three months instead of two, to replacing the calendar-derived contract map with the unconditional roll, to adding month-of-return dummies (not tabulated), and to using last-trade instead of settlement prices (Appendix Table A10).

significant at the 5% level, in the months in which all nine series are observed. The portfolio slope is somewhat below the panel estimate because an equal-weighted position discards the commodity fixed effects and the commodity-specific curve controls; on the same months the panel difference is close to its full-sample value.

The petroleum result is stable over time, and the agricultural result is recent. When the sample is split at January 2008, the crude oil and heating oil slopes are of similar size and significant at the 5% level in both halves, while the agricultural portfolio has a slope close to zero in the first half and of -21.3% per year in the second (Appendix Table A6). This timing is consistent with the integration of grain and energy markets after the mid-2000s, through biofuel mandates and the growth of index investment (Tang and Xiong, 2012). Before 2008 the contrast with metals rests on the petroleum contracts.

Cotton, coffee and sugar have no detectable slope, which is consistent with an ENSO exposure that is tropical and regionally offsetting. Adding them to the weather-sensitive group lowers the difference from metals to -11.6% per year, which remains significant at the 1% level (Appendix Table A5, Panel D). The premium is found in the U.S.-delivered energy and grain contracts.

3.2 Seasons and horizons

ENSO teleconnections over the Americas peak in the boreal winter, which is both the northern heating season and the South American growing season. The predictability is concentrated there. Table 4 splits the ENSO slope by the season of the return month, with the cold season running from November through March. For the six weather-sensitive commodities pooled, the cold-season slope is -21.8% per year and the warm-season slope is -8.1%, and the difference is significant at the 5% level under both asymptotic and bootstrap inference. The cold-season slope is larger in absolute value for each of the six commodities (Figure 3 and Appendix Table A4). The metals show no seasonal pattern, and the difference between the two groups' seasonal contrasts is not significant.

The two weather-sensitive sectors differ in how the season matters. For crude oil and heating oil the slope is significant in both seasons and about twice as large in the cold one. For the grains the response is almost entirely a cold-season one: the cold-season slope is about five times the warm-season slope, and the seasonal difference is significant at the 5% level. This is consistent with a heating-demand channel for energy that operates most strongly in winter and a growing-conditions channel for the grains that is confined to the season of the teleconnection.

If ENSO works through transitory weather shocks, its predictive content should last for months. Table 5 regresses the average excess return over months $t+1$ to $t+h$ on the curve factors and the ENSO state.[9] For the weather-sensitive portfolio the slope falls from -12.2% per year at one month to -4.3% at six months and is close to zero at twelve, and it is significant through three months. The decay is slower for crude oil and heating oil, whose portfolio slope is still significant at the 5% level at twelve months. No metal has a significantly negative slope at any horizon.

The decay does not come from the predictor losing its information, since the ENSO state has a monthly autocorrelation of 0.973. It comes from the response of the premium. A slow-moving risk factor with that persistence would forecast returns at twelve months about as well as at one. A weather shock to a storable good is instead absorbed as inventories adjust, and the premium returns to its usual level within a year for the grains and more slowly for the petroleum contracts.

3.3 El Niño and La Niña

The response comes from La Niña states. The left block of Table 6 reports mean realized returns by ENSO phase, which involve no regression. Crude oil earns 38.9% per year in La Niña months and -19.8% in El Niño months, and heating oil is similar. In neutral months

[9] These regressions use overlapping returns, for which the Newey–West correction is imperfect in small samples (Hodrick, 1992). We read them as a profile of decay.

the return lies between the two, so the ordering follows the state. The weather-sensitive portfolio as a whole earns a positive return in La Niña months and a negative one in El Niño months, and the difference is significant at the 1% level. The metals earn about the same return in every phase.

The right block reports a regression that is piecewise linear in M_t, with separate slopes for negative and positive values of the index. For the weather-sensitive portfolio the slope on negative values is -30.4% per year and the slope on positive values is close to zero, and the test of equal slopes rejects at the 5% level. The gap between the two slopes is largest for crude oil and heating oil, where the La Niña slope is about seven times the El Niño slope. For the grains the two slopes are not statistically different.[10]

This asymmetry is what the convexity of the storage relation implies. When stocks are ample, a change in expected supply has little effect on the marginal value of storage, and the premium barely responds. Near a stockout the same change has a large effect (Deaton and Laroque, 1992; Gorton et al., 2013). La Niña moves the weather-sensitive commodities toward the scarce region, where the premium is sensitive to the state, and El Niño moves them toward the region where it is not. A linear regression on the index averages the two regions, so the full-sample slope of the previous subsections understates the response in La Niña and overstates it in El Niño.

4 A No-Arbitrage Model with Unspanned ENSO

The reduced-form evidence shows that ENSO forecasts returns while being nearly absent from prices. This section develops the smallest no-arbitrage model with that property, following Joslin et al. (2014) as adapted to commodities by Heath (2019) and Jacobs et al. (2017). The model delivers three things the regressions do not: a loading on a true-maturity axis, on which a corn contract thirteen months from delivery and a crude oil contract

[10] Wheat's point estimates run the other way, with the larger slope on the El Niño side. Ubilava (2017) documents El Niño-side asymmetry in wheat prices.

six months from delivery are comparable; an explicit market price of ENSO risk; and a prediction for the whole maturity profile of the ENSO slope, which we test at the end of the section.

4.1 Spanned and unspanned states

A futures price is the expected future spot price net of the premium that long positions earn, $F = \mathbb{E}^{\mathbb{P}}[S] - RP$. If the curve spanned every relevant state, any variable that forecasts the spot price or the premium would be reflected in current prices and would add nothing to a return forecast that conditions on the curve. A state can escape the curve when it moves the two terms of the identity in the same direction. Suppose El Niño is an abundance signal. It lowers the expected future spot price, which pushes F down. It also moves the commodity toward the abundant region of the storage relation, where the premium that long positions require is low, and a lower RP pushes F up. The two effects offset in the price. The premium is the expected return on a long position, so it appears in subsequent returns even though the curve has hardly moved. This is what Duffee (2011) calls a hidden factor.[11]

4.2 Specification

Under the physical measure $\mathbb{P}$, the state $X_t = (L_t', M_t)' \in \mathbb{R}^3$ follows a Gaussian VAR(1),

$$X_{t+1} = K_0^{\mathbb{P}} + K_1^{\mathbb{P}} X_t + \Sigma \varepsilon_{t+1}^{\mathbb{P}}, \qquad \varepsilon_{t+1}^{\mathbb{P}} \sim N(\mathbf{0}, I_3), \tag{4}$$

[11] The offsetting is an average tendency, and it should be weaker where the premium responds less. In line with this, the R^2 of the spanning projection is higher in El Niño months than in La Niña months for each of the six weather-sensitive commodities (Appendix Table A3, Panel A).

partitioned conformably as

$$\begin{pmatrix} L_{t+1} \\ M_{t+1} \end{pmatrix} = \begin{pmatrix} K^{\mathbb{P}}_{0,L} \\ K^{\mathbb{P}}_{0,M} \end{pmatrix} + \begin{pmatrix} K^{\mathbb{P}}_{1,LL} & K^{\mathbb{P}}_{1,LM} \\ K^{\mathbb{P}}_{1,ML} & K^{\mathbb{P}}_{1,MM} \end{pmatrix} \begin{pmatrix} L_t \\ M_t \end{pmatrix} + \Sigma \varepsilon^{\mathbb{P}}_{t+1}. \tag{5}$$

The 2×1 block $K^{\mathbb{P}}_{1,LM}$ measures how much of next month's movement in the curve factors ENSO predicts. Section 2 showed that it differs from zero for corn, crude oil and heating oil.

The stochastic discount factor is exponentially affine with a time-varying price of risk,

$$\mathcal{M}_{t+1} = \exp\left(-r_t - \tfrac{1}{2}\boldsymbol{\lambda}_t'\boldsymbol{\lambda}_t - \boldsymbol{\lambda}_t'\varepsilon^{\mathbb{P}}_{t+1}\right), \qquad \boldsymbol{\lambda}_t = \boldsymbol{\lambda}_0 + \Lambda_1 X_t, \tag{6}$$

the essentially affine specification of Duffee (2002). We order Σ, the Cholesky factor of $\Omega = \Sigma\Sigma'$, with the two curve factors first, so its upper-left block is Σ_L and the L-block of the drift adjustment is $\Sigma_L \boldsymbol{\lambda}_t$ with $\boldsymbol{\lambda}_t \in \mathbb{R}^2$; Λ_1 is 2×3. Only these two shocks are priced by futures, because futures prices depend only on L_t. Under $\mathbb{Q}$,

$$L_{t+1} = K^{\mathbb{Q}}_0 + K^{\mathbb{Q}}_1 L_t + \Sigma_L \varepsilon^{\mathbb{Q}}_{t+1}, \tag{7}$$

with the two measures linked by

$$K^{\mathbb{Q}}_0 = K^{\mathbb{P}}_{0,L} - \Sigma_L \boldsymbol{\lambda}_0, \qquad \begin{pmatrix} K^{\mathbb{Q}}_1 & \mathbf{0} \end{pmatrix} = \begin{pmatrix} K^{\mathbb{P}}_{1,LL} & K^{\mathbb{P}}_{1,LM} \end{pmatrix} - \Sigma_L \Lambda_1. \tag{8}$$

The defining restriction is the zero in the last block: M_t does not enter the $\mathbb{Q}$-dynamics of L_t, and hence does not enter the pricing equation. Reading off the ENSO column,

$$\Lambda_{1,M} = \Sigma_L^{-1} K^{\mathbb{P}}_{1,LM}, \tag{9}$$

so the market price of ENSO risk is identified from the physical dynamics alone. In

words, the market prices futures as if ENSO did not help forecast the curve factors, while under the physical measure it does. The wedge between the two sets of dynamics is the compensation for risk, and equation (9) attributes the part of it that moves with ENSO to a price of risk that is linear in the ENSO state. We impose the restriction on the basis of the spanning evidence in Table 1; the estimation is in two steps and does not test it against a spanned alternative.

Log futures prices are affine in the pricing factors. Writing τ for months to expiry,

$$f_t^{(n)} = A_{\tau_{t,n}} + \boldsymbol{B}'_{\tau_{t,n}} L_t + \eta_t^{(n)}, \qquad \eta_t^{(n)} \sim N(0, \sigma_\eta^2), \tag{10}$$

with the Riccati recursions

$$\boldsymbol{B}_\tau = (K_1^{\mathbb{Q}})' \boldsymbol{B}_{\tau-1}, \tag{11}$$

$$A_\tau = A_{\tau-1} + \boldsymbol{B}'_{\tau-1} K_0^{\mathbb{Q}} + \tfrac{1}{2} \boldsymbol{B}'_{\tau-1} \Omega_L \boldsymbol{B}_{\tau-1}, \tag{12}$$

and initial conditions $\boldsymbol{B}_0 = \boldsymbol{\rho}_1$, $A_0 = \rho_0$. Substituting (10) into the expected excess return and using (11) and (12) gives (Appendix A)

$$\mathbb{E}_t^{\mathbb{P}}\left[rx_{t+1}^{(\tau)}\right] = \underbrace{\boldsymbol{B}'_{\tau-1}\left(K_{0,L}^{\mathbb{P}} - K_0^{\mathbb{Q}}\right) - \tfrac{1}{2}\boldsymbol{B}'_{\tau-1}\Omega_L \boldsymbol{B}_{\tau-1}}_{\text{constant}} + \underbrace{\boldsymbol{B}'_{\tau-1}\left(K_{1,LL}^{\mathbb{P}} - K_1^{\mathbb{Q}}\right) L_t}_{\text{curve component}} + \underbrace{\boldsymbol{B}'_{\tau-1} K_{1,LM}^{\mathbb{P}} M_t}_{\text{ENSO component}}. \tag{13}$$

The coefficient $\boldsymbol{B}'_{\tau-1} K_{1,LM}^{\mathbb{P}}$, annualized, is the ENSO loading at maturity τ, the structural counterpart of the reduced-form β_M. Writing RP_t^{tv} for the sum of the two time-varying components, we also report the covariance-based contribution

$$\text{ENSO share} = \frac{\operatorname{Cov}\left(\boldsymbol{B}'_{\tau-1} K_{1,LM}^{\mathbb{P}} M_t,\ RP_t^{tv}\right)}{\operatorname{Var}(RP_t^{tv})} \times 100, \tag{14}$$

so that the ENSO and curve shares sum to 100%. Because the two components are negatively correlated for all nine commodities, a ratio of variances would not sum to 100%.

The three terms of equation (13) have a direct reading. The constant is the unconditional premium at maturity τ. The curve component is the time variation that a model with full spanning would also deliver, since it depends only on the current curve. The ENSO component is zero under spanning. It is present when ENSO forecasts the curve factors under the physical measure while being excluded from their risk-neutral dynamics, and its size at each maturity is governed by the pricing loadings $\boldsymbol{B}_{\tau-1}$.

Estimation is in two steps, as in Joslin et al. (2011) and Heath (2019): the full-state VAR (4) by OLS on calendar-consecutive month pairs, then the risk-neutral parameters by maximum likelihood on (10). We parametrize $K_1^{\mathbb{Q}}$ so that it is stationary by construction, and we treat the curve factors as observed regressors while fitting all seven prices with an i.i.d. measurement error. Appendix B gives the details. The block $K_{1,LM}^{\mathbb{P}}$ comes from the time-series VAR and $\boldsymbol{B}_{\tau-1}$ from the cross-sectional fit, so the sign and the predictive content of the estimated premium come from the time series.

4.3 Estimates and the maturity profile

Two factors price the curves closely. The average root mean squared pricing error is 0.42% of the log price for crude oil and below 2.2% for every commodity except natural gas, whose seasonal curve two factors cannot capture (Appendix Table A1, Panel A). The no-arbitrage restrictions cost little relative to an unrestricted two-factor benchmark.[12]

The market price of ENSO risk has the sign of the reduced-form slopes. The price of level-factor risk per unit of ENSO is negative for all six weather-sensitive commodities, about -0.2 for crude oil and heating oil, and close to zero for gold and silver (Appendix Table A1, Panel C). A higher ENSO state lowers the compensation that the market requires for bearing shocks to the level of the curve, which is the model's expression of a smaller premium in a state of abundance.

[12] Allowing a deterministic delivery-month seasonal lowers the natural gas error from 4.5% to 2.7% and moves the ENSO loadings by 0.1 percentage points per year at the median and by 2.1 for natural gas (Appendix Table A9).

The model-implied loadings match the reduced-form slopes. Table 7 reports the decomposition of the premium at a true maturity of two months. A 1°C higher ONI lowers the expected excess return by 23.5% per year for crude oil, by nearly the same amount for heating oil, and by between 8.0% and 15.3% for natural gas and the grains. The loadings for the metals are small, and those for gold and silver are positive. The correlation with the slopes of Table 2 is 0.99 across the nine commodities. The model loading is built from the same curve factors and the same VAR as the regression, so this agreement holds by construction at a single maturity. What the model adds is the profile across maturities.

The loadings are stated at a common maturity, which the reduced-form slopes are not. The second nearby contract is two months from expiry for the energy commodities and the metals and, on average, between three and four months for the grains (Table 1). The loadings are not sensitive to the calendar used to place contracts on the maturity axis: under the simpler convention that the n-th nearby has n months to expiry, they differ from the baseline by at most 0.23 (Appendix Table A2, Panel B).

The unspanned state accounts for a large part of the variation in the premium. For crude oil the model-implied premium has a standard deviation of 21.5% per year, of which the ENSO component contributes 19.8% and the curve component 13.7%. The ENSO component is the larger of the two for corn, soybeans, crude oil and heating oil, and it accounts for most of the variation in their premium. Where the curve component is large, as for natural gas, the share of ENSO is small, so the loading is the better summary of its role.

The loading declines in absolute value with maturity for every weather-sensitive commodity. For crude oil it falls from -23.5% per year at two months to -15.4% at eight months (Appendix Table A2). The decline comes from the risk-neutral transition matrix, through the recursion $\boldsymbol{B}_\tau = (K_1^{\mathbb{Q}})'\boldsymbol{B}_{\tau-1}$. The persistence of ENSO cannot produce it: the autoregressive coefficient of the ENSO state is between 0.97 and 0.98 in every system, and a mechanism running through it would generate a nearly flat profile. The market prices the

curve shocks that ENSO forecasts as mean-reverting, which is a Samuelson (1965) effect.[13]

The maturity profile is an over-identifying restriction that the reduced form does not impose. We estimate a separate ENSO slope for each of rx_2 through rx_6 from the same regressors with a joint Newey–West covariance, place each contract at its mean true months to expiry, and test whether the model's profile passes through the five estimates. The test is on the shape: the four slopes relative to rx_2, which the model predicts from $K_1^{\mathbb{Q}}$ alone. Figure 4 shows the comparison for heating oil, crude oil and corn. In each panel the freely estimated slopes shrink toward zero as maturity lengthens, and the model's profile lies within one standard error of every one of them. The shape restriction is not rejected for any of the nine commodities: the largest test statistic is 6.75, for corn, against a 5% critical value of 9.49 (Appendix Table A2, Panel C).[14]

5 Interpretation

The model attributes the predictability to a premium that varies with the ENSO state. A premium on a risk specific to a handful of commodity markets need not come from a covariance with aggregate consumption. In the theory of storage the marginal agent is the inventory-holding intermediary, whose capacity to absorb hedging demand is limited when stocks are tight, so the compensation is for storage and hedging-pressure risk (Fama and French, 1987; Bessembinder, 1992; Gorton et al., 2013). In a scarce state the theory predicts more hedging demand, less capacity to meet it and a higher premium for the long side; in an abundant state both forces relax.

This interpretation makes three predictions that do not involve returns. If ENSO moves commodities between abundance and scarcity, the positions of commercial hedgers should

[13]For corn, copper and silver the estimated spectral radius of $K_1^{\mathbb{Q}}$ is at the boundary of the stationary region. For corn this affects only the level eigenvalue, and the profile still declines by about a fifth across the maturity range. The copper and silver profiles are flat.

[14]The reduced-form slopes against which the profile is measured have standard errors between 2.3% and 11.4% per year, so the test is informative about departures of that size.

move with it. The futures basis, which is the curve's own measure of scarcity, should respond in the same month. And the physical quantities through which the weather acts, heating demand and inventories, should connect the ENSO state to prices. This section presents evidence on each and then considers an alternative interpretation.

5.1 Hedging pressure

A higher value of hedging pressure means that producers are hedging more heavily, and the theory of storage predicts a higher premium to the long side. Hedging pressure is higher in La Niña than in El Niño for each of the six weather-sensitive commodities (Table 8, Panel A, and Figure 5). Pooling the six, mean hedging pressure rises from 0.014 of open interest in El Niño months to 0.066 in La Niña months, and the gap has a t-statistic of 2.95. For the three metals pooled the gap is small and insignificant. La Niña is the state in which producers hedge more heavily, and it is the state in which Table 6 shows realized returns to be highest.

The response is graded in the ENSO state as well as different across phases. In a panel regression on the continuous index, hedging pressure in the weather-sensitive commodities falls by 0.024 of open interest per 1°C, significant at the 1% level, and the response of the metals is close to zero. The gap between phases is widest for soybeans, corn and heating oil. Hedging pressure has a large commodity-specific mean, so the difference between the two groups' responses is estimated less precisely than the difference in return slopes, and it is not statistically significant.

ENSO is not a proxy for positioning. If ENSO forecast returns only because it is correlated with positions, its slope would fall once positions are controlled for. Panel B adds hedging pressure and the speculative net position to the return regression, with both specifications estimated on the same window. The ENSO slopes of the three energy commodities, corn and soybeans change by about one percentage point or less, and the coefficient on hedging pressure is not significant for any of the five. Wheat is the exception;

its slope more than doubles when the controls enter. ENSO and positions are complements. The first is an exogenous state that shifts the quantity of risk to be borne, and the second records who bears it.

5.2 The basis and the physical links

If El Niño moves weather-sensitive commodities toward abundance, it should tilt their curves toward contango in the same month. Table 3, Panel C reports the panel regression of the basis on the ENSO state, and Appendix Table A7 the commodity detail.[15] A 1°C higher index lowers the basis of the weather-sensitive commodities by 3.0% per year, significant at the 5% level, and has no effect on the basis of the metals. The response is largest for the energy contracts, at about 4.5% per year for crude oil and heating oil.

The basis is part of the curve, so this response is the small spanned part of ENSO seen through one of its components. Per 1°C, ENSO moves the basis by 3% per year and the expected return by about 16%. The curve registers the direction of the shock and little of its size.

The physical quantities through which the weather acts are strongly related to prices and weakly related to ENSO (Appendix Table A8). In cold months a heating-degree-day anomaly that is 100 degree days higher raises the one-month excess return on natural gas by 122.9% per year, and it raises the return on heating oil as well. Inventories move the basis as the theory of storage requires: a one-standard-deviation higher stock of distillates lowers the heating oil basis by 10.2% per year, and natural gas storage has a similar effect on the gas basis. All four estimates are significant at the 1% level.

The link from ENSO to these quantities has the predicted sign in every specification. ENSO lowers national heating degree days significantly in the contemporaneous deep-winter months, and its effects on degree days at other horizons and on inventories are

[15] These regressions include no curve factors, because the basis is a linear combination of two points on the same curve and the factors explain a median 96% of it.

not significant. The teleconnection over the United States is dipolar, warm in the north and cool in the south, so a national degree-day aggregate measures it with noise. The evidence from physical quantities therefore supports the storage interpretation for the energy commodities through its second link, from the physical state to prices.

Our results are complementary to Cashin et al. (2017), who find that El Niño raises many commodity prices on impact. That literature measures the contemporaneous response of the price level. We condition on the current curve, which already embeds whatever repricing has occurred, and ask about subsequent expected returns. A commodity can rise on impact and still offer a lower expected return if the shock has moved it into a state of abundance.

5.3 An alternative interpretation

Within a no-arbitrage model, predictable excess returns are premia by construction. An alternative is that the predictability reflects the slow diffusion of public climate information into prices. Under that view the market underreacts to the ENSO state, prices drift in the direction of the news, and returns are predictable without any compensation for risk.

Five findings are easier to reconcile with a premium. The effect is absent in metals, which trade on the same exchanges and receive the same information. It is concentrated in the season of the physical teleconnection. The response is asymmetric across El Niño and La Niña, which the convexity of storage predicts and slow diffusion does not. The basis moves in the same month, so the small part of ENSO that the curve reflects is not delayed. And hedging pressure moves with the same state. These findings favor the premium interpretation, and they do not exclude a role for slow diffusion.

6 Conclusion

ENSO is almost absent from commodity futures curves, and it forecasts the returns on the commodities whose storage state it shifts. A 1°C higher ONI lowers expected one-month excess returns on weather-sensitive commodities by about 16% per year and leaves the metals unaffected. The predictability is concentrated in the cold season, at horizons of a few months and in La Niña states, and it comes with a tilt in the basis and a shift in the positions of commercial hedgers. These patterns are consistent with a storage premium: if ENSO moves the expected spot price and the premium in the same direction, the two offset in the futures price and the premium appears in subsequent returns. A no-arbitrage model in which ENSO enters the physical dynamics and is excluded from the pricing equation implies a premium that declines with maturity, and the data do not reject that profile.

Because the curve does not encode the ENSO state, a hedging or risk-management model calibrated only to curve dynamics misstates expected returns for these commodities in the months when the climate signal is strongest. More generally, a climate state can matter for a market without being visible in its prices, which is a reason to look for physical climate risk in expected returns as well as in prices. If extreme El Niño events become more frequent under greenhouse warming (Cai et al., 2014), the premium documented here will matter more.

References

Ang, A. and Piazzesi, M. (2003). A no-arbitrage vector autoregression of term structure dynamics with macroeconomic and latent variables. *Journal of Monetary Economics*, 50(4):745–787.

Baldauf, M., Garlappi, L., and Yannelis, C. (2020). Does climate change affect real estate prices? Only if you believe in it. *The Review of Financial Studies*, 33(3):1256–1295.

Barnett, M., Brock, W., and Hansen, L. P. (2020). Pricing uncertainty induced by climate change. *The Review of Financial Studies*, 33(3):1024–1066.

Bessembinder, H. (1992). Systematic risk, hedging pressure, and risk premiums in futures markets. *The Review of Financial Studies*, 5(4):637–667.

Brunner, A. D. (2002). El Niño and world primary commodity prices: Warm water or hot air? *Review of Economics and Statistics*, 84(1):176–183.

Cai, W., Borlace, S., Lengaigne, M., van Rensch, P., Collins, M., Vecchi, G., Timmermann, A., Santoso, A., McPhaden, M. J., Wu, L., England, M. H., Wang, G., Guilyardi, E., and Jin, F.-F. (2014). Increasing frequency of extreme El Niño events due to greenhouse warming. *Nature Climate Change*, 4:111–116.

Cashin, P., Mohaddes, K., and Raissi, M. (2017). Fair weather or foul? The macroeconomic effects of El Niño. *Journal of International Economics*, 106:37–54.

Deaton, A. and Laroque, G. (1992). On the behaviour of commodity prices. *The Review of Economic Studies*, 59(1):1–23.

Driscoll, J. C. and Kraay, A. C. (1998). Consistent covariance matrix estimation with spatially dependent panel data. *The Review of Economics and Statistics*, 80(4):549–560.

Duffee, G. R. (2002). Term premia and interest rate forecasts in affine models. *The Journal of Finance*, 57(1):405–443.

Duffee, G. R. (2011). Information in (and not in) the term structure. *The Review of Financial Studies*, 24(9):2895–2934.

Fama, E. F. and French, K. R. (1987). Commodity futures prices: Some evidence on forecast power, premiums, and the theory of storage. *The Journal of Business*, 60(1):55–73.

Giglio, S., Kelly, B., and Stroebel, J. (2021). Climate finance. *Annual Review of Financial Economics*, 13:15–36.

Gorton, G., Hayashi, F., and Rouwenhorst, K. G. (2013). The fundamentals of commodity futures returns. *Review of Finance*, 17(1):35–105.

Heath, D. (2019). Macroeconomic factors in oil futures markets. *Management Science*, 65(9):4407–4421.

Hodrick, R. J. (1992). Dividend yields and expected stock returns: Alternative procedures for inference and measurement. *The Review of Financial Studies*, 5(3):357–386.

Ibragimov, R. and Müller, U. K. (2010). t-statistic based correlation and heterogeneity robust inference. *Journal of Business & Economic Statistics*, 28(4):453–468.

Iizumi, T., Luo, J.-J., Challinor, A. J., Sakurai, G., Yokozawa, M., Sakuma, H., Brown, M. E., and Yamagata, T. (2014). Impacts of El Niño Southern Oscillation on the global yields of major crops. *Nature Communications*, 5:3712.

Jacobs, K., Li, B., and Pirrong, C. (2017). Supply and demand in electricity futures: Identification through the term structure. Working paper.

Joslin, S., Priebsch, M., and Singleton, K. J. (2014). Risk premiums in dynamic term structure models with unspanned macro risks. *The Journal of Finance*, 69(3):1197–1233.

Joslin, S., Singleton, K. J., and Zhu, H. (2011). A new perspective on Gaussian dynamic term structure models. *The Review of Financial Studies*, 24(3):926–970.

Newey, W. K. and West, K. D. (1987). A simple, positive semi-definite, heteroskedasticity and autocorrelation consistent covariance matrix. *Econometrica*, 55(3):703–708.

Samuelson, P. A. (1965). Proof that properly anticipated prices fluctuate randomly. *Industrial Management Review*, 6(2):41–49.

Stambaugh, R. F. (1999). Predictive regressions. *Journal of Financial Economics*, 54(3):375–421.

Szymanowska, M., de Roon, F., Nijman, T., and van den Goorbergh, R. (2014). An anatomy of commodity futures risk premia. *The Journal of Finance*, 69(1):453–482.

Tang, K. and Xiong, W. (2012). Index investment and the financialization of commodities. *Financial Analysts Journal*, 68(6):54–74.

Ubilava, D. (2017). The ENSO effect and asymmetries in wheat price dynamics. *World Development*, 96:490–502.

Ubilava, D. (2018). The role of El Niño Southern Oscillation in commodity price movement and predictability. *American Journal of Agricultural Economics*, 100(1):239–263.

Table 1: Samples, curve factors and the spanning of ENSO

Month-end settlement samples on a complete monthly grid. $\bar{\tau}_2$ is the average months to expiry of the second nearby contract implied by the exchange delivery cycle; it equals 2.0 for the three NYMEX energy chains and copper, which list every calendar month. PC1 and PC2 are the shares of the cross-sectional variance of the seven demeaned log futures prices explained by the first two principal components. The last two columns report the projection $M_t = \alpha + \gamma_1 PC_t^1 + \gamma_2 PC_t^2 + UM_t$: R^2 is the share of ENSO variation spanned by the curve and "Unspanned" is $(1 - R^2) \times 100$. The factor-by-factor and phase-by-phase decomposition is in Appendix Table A3.

Commodity	Sector	Start	End	T	$\bar{\tau}_2$	PC1 (%)	PC2 (%)	$R^2(M$ on $L)$	Unspanned (%)
Corn	Agri.	1990-05	2026-03	405	4.2	98.67	1.00	0.048	95.2
Soybeans	Agri.	1990-01	2026-03	435	3.2	99.32	0.53	0.023	97.7
Wheat	Agri.	1992-03	2026-03	352	4.2	98.51	1.29	0.024	97.6
Crude Oil	Energy	1990-01	2026-03	435	2.0	99.81	0.18	0.085	91.5
Heating Oil	Energy	1990-01	2026-03	435	2.0	99.74	0.22	0.056	94.4
Natural Gas	Energy	1990-04	2026-03	432	2.0	97.43	1.71	0.075	92.5
Copper	Metals	1990-01	2026-03	435	2.0	99.96	0.04	0.017	98.3
Gold	Metals	1990-01	2026-03	435	2.0	99.99	0.01	0.004	99.6
Silver	Metals	1990-01	2026-03	435	2.0	99.99	0.01	0.026	97.4

Table 2: ENSO predicts commodity futures excess returns

β_M from equation (3), estimated separately for each commodity and for the second, third and sixth nearby contracts, in percent per year per 1°C of ONI. The first three columns give the number of return observations and the mean and standard deviation of rx_2 over that sample; the number of observations is smaller than the number of full-curve months in Table 1, because a return needs two consecutive observed months. t-statistics use Newey–West standard errors with 12 lags; ΔR^2 is the increment from adding M_t to a regression on L_t alone.

		rx_2 descriptives			rx_2			rx_3			rx_6		
Commodity	Sector	T	Mean	S.D.	β_M	t	ΔR^2	β_M	t	ΔR^2	β_M	t	ΔR^2
Corn	Agri.	400	−6.5	86.9	−13.5	−2.70	0.017	−13.2	−2.78	0.018	−9.2	−2.30	0.013
Soybeans	Agri.	434	2.5	78.3	−6.6	−1.50	0.005	−6.5	−1.49	0.005	−5.7	−1.44	0.005
Wheat	Agri.	349	−11.0	98.3	−6.9	−1.47	0.003	−8.3	−1.87	0.005	−9.5	−2.56	0.010
Crude Oil	Energy	434	2.7	125.1	−23.9	−3.37	0.024	−21.3	−3.41	0.023	−17.2	−3.22	0.021
Heating Oil	Energy	434	8.9	122.1	−26.8	−3.89	0.032	−22.2	−3.63	0.027	−18.6	−3.53	0.026
Natural Gas	Energy	431	−21.5	172.7	−15.9	−1.39	0.006	−14.9	−1.50	0.006	−8.9	−1.15	0.004
Copper	Metals	434	5.5	85.9	−5.5	−1.34	0.003	−5.3	−1.32	0.003	−4.8	−1.25	0.002
Gold	Metals	434	3.8	53.2	2.0	0.89	0.001	2.0	0.86	0.001	1.9	0.85	0.001
Silver	Metals	434	4.1	99.5	1.4	0.31	0.000	1.5	0.33	0.000	1.1	0.24	0.000

Table 3: Sector portfolios, the weather-sensitive-versus-metals panel, and the basis

Panel A: equal-weighted second-nearby excess returns of each sector portfolio on M_t and the members' averaged standardized curve factors; a portfolio is defined only in months when every member is observed. **Panel B**: the stacked nine-commodity panel of Section 3 with commodity fixed effects, commodity-specific curve slopes, and M_t interacted with a weather-sensitive indicator; the indented rows re-estimate the interaction on the 348 months in which the balanced long–short exists and report the two long–short variants. **Panel C**: the same specification for the contemporaneous basis. Driscoll–Kraay standard errors (Bartlett, 12 lags); "Boot. p" is a 24-month circular moving-block bootstrap with 4,999 draws. All slopes are percent per year per 1°C of ONI. Panel B components are rounded independently; the unrounded metals and interaction estimates, -0.67 and -15.11, sum to the weather-sensitive slope of -15.79.

Row	β_M	t	Boot. p	R^2 / ΔR^2	Obs.
Panel A: equal-weighted sector portfolios of rx_2					
Agriculture	-8.7	-2.06	—	0.008	348
Energy	-22.1	-3.23	—	0.026	431
Energy ex. nat. gas	-25.1	-3.74	0.003	0.029	434
Weather-sensitive	-12.2	-3.01	0.020	0.017	348
Metals	-0.4	-0.14	—	0.000	434
Weather-sens. − metals	-14.0	-2.53	—	0.017	348
Panel B: stacked panel of rx_2, Driscoll–Kraay standard errors					
Metals (β_M)	-0.7	-0.23	0.817		3,784
Weather-sensitive − metals (δ_M)	-15.1	-3.25	0.012		
Weather-sensitive ($\beta_M + \delta_M$)	-15.8	-3.72	0.005	0.027	
δ_M on the long–short months only	-16.2	-3.25	—		3,132
Long–short portfolio, same months	-14.0	-2.53	—		348
Long–short, available members, full sample	-12.6	-2.59	—		434
Panel C: stacked panel of the contemporaneous basis, Driscoll–Kraay standard errors					
Metals (β_M^{con})	-0.0	-0.16	—		3,799
Weather-sensitive − metals	-3.0	-2.22	—		
Weather-sensitive	-3.0	-2.31	—	0.084	

Table 4: Cold versus warm season: panel test

Driscoll–Kraay panel regressions of the second-nearby excess return on $M_t \times$ cold and $M_t \times$ warm, where cold means the return month falls in November–March. The pooled rows come from the single nine-commodity panel in which M_t is interacted with season and with a weather-sensitive indicator; the difference-in-differences is the extra seasonal contrast of the weather-sensitive group relative to metals. "Diff." is $\beta_M^c - \beta_M^w$ with a Wald p-value from the Driscoll–Kraay covariance. The last five rows vary the inference for the weather-sensitive panel: the point estimate is invariant, the asymptotic p-value ranges from 0.010 to 0.042 across lag lengths, and the block bootstrap gives $p = 0.015$. All estimates are percent per year per 1°C of ONI.

		Cold (Nov–Mar)		Warm (Apr–Oct)		Cold − warm		
Panel	Obs.	β_M^c	t	β_M^w	t	Diff.	t	p
Weather-sensitive (6)	2,482	−21.8	−4.08	−8.1	−1.66	−13.7	−2.29	0.022
Metals (3)	1,302	−3.1	−0.92	3.0	0.55	−6.1	−0.89	0.376
Agriculture (3)	1,183	−13.8	−3.32	−2.7	−0.50	−11.0	−2.02	0.043
Energy ex. nat. gas (2)	868	−32.8	−3.46	−15.6	−2.22	−17.2	−1.63	0.103
Pooled panel with weather-sensitive interactions								
Weather-sensitive	3,784	−21.8	−4.08	−8.1	−1.66	−13.7	−2.29	0.022
Metals	3,784	−3.1	−0.92	3.0	0.55	−6.1	−0.89	0.376
Difference-in-differences						−7.6	−0.98	0.326
Weather-sensitive cold − warm: inference robustness								
Driscoll–Kraay, 6 lags						−13.7	−2.03	0.042
Driscoll–Kraay, 12 lags						−13.7	−2.29	0.022
Driscoll–Kraay, 18 lags						−13.7	−2.58	0.010
Block bootstrap, 24-month blocks						−13.7	—	0.015
Block bootstrap, 36-month blocks						−13.7	—	0.015

Table 5: Multi-horizon predictability

β_M from regressions of the average annualized second-nearby excess return over months $t+1$ through $t+h$ on the curve factors L_t and M_t. Because the dependent variable is an average of already annualized returns, slopes are comparable across horizons; all are percent per year per 1°C of ONI. t-statistics use Newey–West standard errors with $\max(12, h+1)$ lags on overlapping observations. At $h = 12$ silver and the metals portfolio have significantly positive slopes.

	$h=1$		$h=3$		$h=6$		$h=12$	
Commodity / portfolio	β_M	t	β_M	t	β_M	t	β_M	t
Corn	−13.5	−2.70	−10.7	−2.30	−7.1	−1.64	0.3	0.09
Soybeans	−6.6	−1.50	−4.3	−1.11	−1.5	−0.45	0.5	0.15
Wheat	−6.9	−1.47	−1.9	−0.44	3.2	0.63	5.9	1.21
Crude Oil	−23.9	−3.37	−23.8	−3.44	−17.2	−2.90	−10.0	−1.77
Heating Oil	−26.8	−3.89	−25.3	−3.85	−19.5	−3.09	−13.9	−2.20
Natural Gas	−15.9	−1.39	−14.9	−1.51	−12.2	−1.52	−4.5	−0.66
Copper	−5.5	−1.34	−2.7	−0.73	1.4	0.38	4.6	1.22
Gold	2.0	0.89	2.5	1.28	2.7	1.59	2.9	1.86
Silver	1.4	0.31	3.2	0.76	5.2	1.41	7.6	2.54
Weather-sensitive	−12.2	−3.01	−8.9	−2.46	−4.3	−1.26	0.2	0.05
Energy ex. nat. gas	−25.1	−3.74	−24.3	−3.75	−18.0	−3.06	−11.9	−2.03
Metals	−0.4	−0.14	1.2	0.48	3.4	1.28	5.3	2.11

Table 6: Realized returns by ENSO phase and piecewise slopes

The left block reports mean *realized* annualized second-nearby excess returns unconditionally and in El Niño months ($M_t > 0.5$°C), neutral months and La Niña months ($M_t < -0.5$°C), with the number of months in each phase. "Diff." is the El Niño mean minus the La Niña mean, with a Newey–West Wald test on phase dummies (12 lags). The right block reports $rx_{2,t+1} = \alpha + \boldsymbol{\beta}_{pc}' L_t + \beta^+ \max(M_t, 0) + \beta^- \min(M_t, 0) + \varepsilon_{t+1}$, in percent per year per 1°C, with t_{sym} the test of $\beta^+ = \beta^-$.

	Mean realized rx_2 (%/yr)				Months			El Niño − La Niña		Piecewise		
Unit	All	El Niño	Neutral	La Niña	El	Ne	La	Diff.	t	β^+	β^-	t_{sym}
Corn	−6.5	−19.9	−7.5	6.1	98	184	118	−26.0	−2.37	−5.7	−24.8	1.06
Soybeans	2.5	−3.8	2.5	8.3	110	206	118	−12.1	−1.38	−2.1	−13.1	0.73
Wheat	−11.0	−25.3	−2.3	−13.1	81	158	110	−12.2	−1.36	−15.9	5.1	−1.30
Crude Oil	2.7	−19.8	−5.9	38.9	110	206	118	−58.7	−3.82	−6.6	−48.4	1.87
Heating Oil	8.9	−17.6	0.3	48.5	110	206	118	−66.1	−3.84	−7.6	−54.6	1.91
Natural Gas	−21.5	−27.4	−21.5	−16.2	110	203	118	−11.3	−0.43	−4.0	−32.8	0.88
Copper	5.5	−4.2	9.6	7.4	110	206	118	−11.6	−1.14	−4.5	−6.9	0.16
Gold	3.8	6.1	3.7	1.6	110	206	118	4.5	0.82	2.1	2.0	0.01
Silver	4.1	6.3	3.4	3.1	110	206	118	3.2	0.32	7.7	−7.8	0.83
Weather-sensitive	−2.5	−17.4	−5.8	13.1	80	158	110	−30.6	−2.71	2.2	−30.4	2.50
Energy ex. nat. gas	5.8	−18.7	−2.8	43.7	110	206	118	−62.4	−3.98	−6.9	−51.2	1.97
Agriculture	−4.5	−16.7	−1.7	0.4	80	158	110	−17.2	−1.99	−6.4	−11.6	0.36
Metals	4.4	2.7	5.6	4.0	110	206	118	−1.3	−0.20	1.2	−2.7	0.36

Table 7: Decomposition of the model-implied risk premium

Decomposition of the model-implied expected one-month excess return at a true maturity of $\tau = 2$ months, following equation (13); all quantities annualized percent. "Curve s.d." and "ENSO s.d." are the standard deviations of $\boldsymbol{B}'_{\tau-1}(K^{\mathbb{P}}_{1,LL} - K^{\mathbb{Q}}_{1})L_t$ and $\boldsymbol{B}'_{\tau-1}K^{\mathbb{P}}_{1,LM}M_t$, and "Corr." is their correlation; because they are negatively correlated for all nine commodities, a component standard deviation can exceed that of the total premium. "ENSO loading" is $\boldsymbol{B}'_{\tau-1}K^{\mathbb{P}}_{1,LM}$ in percent per year per 1°C, and "Range over near-best" is its range over all starting values whose log-likelihood is within 0.5 of the best (a point where only one start qualifies). "ENSO share" is the covariance-based contribution (14), so the ENSO and curve shares sum to 100%; it is sensitive to the size of the curve component in the denominator, which is why natural gas records 5.3% with a loading of -12.9.

	Total premium		Components					
Commodity	Mean	S.D.	Curve s.d.	ENSO s.d.	Corr.	ENSO loading	Range over near-best	ENSO share (%)
Corn	−7.0	13.0	4.8	13.1	−0.22	−15.3	[-15.3, -15.3]	94.5
Soybeans	2.8	7.4	3.9	6.7	−0.12	−8.0	[-8.0, -8.0]	77.4
Wheat	−11.0	12.8	11.6	7.1	−0.13	−8.5	[-8.5, -8.5]	24.0
Crude Oil	3.6	21.5	13.7	19.8	−0.21	−23.5	[-23.5, -23.5]	72.1
Heating Oil	6.6	19.7	8.5	19.7	−0.22	−23.4	[-23.4, -23.4]	90.7
Natural Gas	−19.8	26.6	27.4	10.9	−0.27	−12.9	[-12.9, -12.9]	5.3
Copper	5.3	8.5	7.7	4.3	−0.09	−5.1	[-5.1, -5.1]	21.1
Gold	3.7	5.0	4.8	1.6	−0.06	2.0	[2.0, 2.0]	8.9
Silver	3.8	1.7	1.4	1.1	−0.16	1.3	[1.3, 1.3]	36.8

Table 8: Hedging pressure and ENSO

Hedging pressure is (commercial short − commercial long) / open interest from the CFTC legacy futures-only Commitments of Traders reports, last report of each month, stamped by release month. **Panel A** reports its mean by ENSO phase, the La Niña minus El Niño gap and a t-statistic; the two panel rows pool the six weather-sensitive commodities and the three metals with Driscoll–Kraay standard errors, and the indented row is the difference between the two groups' responses to the continuous index M_t. **Panel B** adds hedging pressure and the speculative net position to the return regression (3). Both β_M columns are estimated on the same COT window, so the comparison isolates the controls rather than the sample: β_M without controls, β_M with them, and the coefficient on hedging pressure. T is that window, which begins in 1995 for energy, metals and softs and in 1998 for the CBOT grains.

Panel A: hedging pressure (commercial net short as a share of open interest) by ENSO phase

Commodity	El Niño	Neutral	La Niña	La − El	t
Corn	−0.006	0.018	0.076	0.082	1.84
Soybeans	0.002	0.068	0.118	0.116	2.52
Wheat	−0.051	−0.047	−0.011	0.040	1.21
Crude Oil	0.102	0.096	0.107	0.005	0.15
Heating Oil	0.056	0.076	0.121	0.065	3.19
Natural Gas	−0.033	−0.021	−0.019	0.014	0.35
Copper	0.010	0.075	0.088	0.078	1.42
Gold	0.279	0.333	0.248	−0.031	−0.33
Silver	0.366	0.367	0.352	−0.014	−0.32
Weather-sensitive (6), panel	0.014	0.033	0.066	0.052	2.95
Metals (3), panel	0.218	0.258	0.229	0.011	0.29
HP on M_t: WS − metals				−0.0194	−1.26

Panel B: rx_2 on M_t with and without the positioning controls, both columns on the COT window

	Without controls		With HP and spec. net		HP coefficient		
Commodity	β_M	t	β_M	t	β	t	T
Corn	−14.0	−2.66	−14.7	−3.07	83.7	0.78	338
Soybeans	−5.8	−1.18	−5.2	−1.01	−74.1	−0.97	338
Wheat	−6.0	−1.23	−14.3	−2.89	−437.8	−2.74	326
Crude Oil	−23.4	−3.17	−22.8	−3.15	253.8	0.88	374
Heating Oil	−26.0	−3.81	−26.8	−3.80	−239.6	−1.13	374
Natural Gas	−16.7	−1.45	−15.5	−1.43	135.6	0.42	374
Copper	−5.3	−1.28	−5.4	−1.20	18.2	0.14	374
Gold	2.9	1.16	2.8	1.21	−7.4	−0.12	374
Silver	3.0	0.60	3.0	0.57	−26.7	−0.21	374

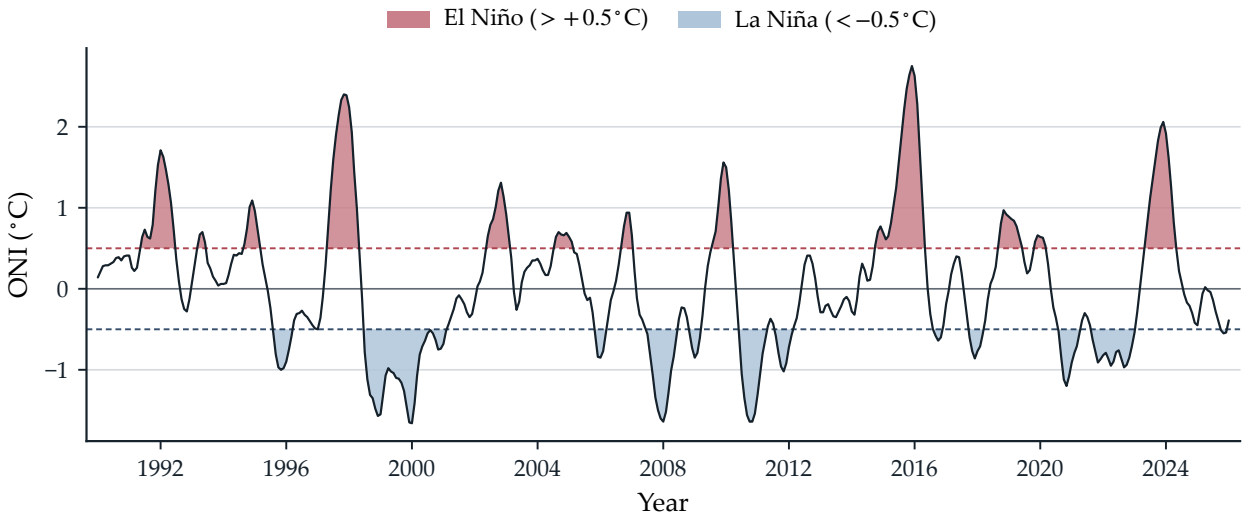


Figure 1: The ENSO state, 1990–2026. The Oceanic Niño Index over the estimation sample. Throughout the paper the color key is: red = El Niño / warm season / energy, navy = La Niña / cold season / agriculture, gray = neutral phase, metals placebo and model curves. Here the darker red shading marks El Niño months (ONI above $+0.5$°C) and the lighter blue shading La Niña months (ONI below -0.5°C); the red tint is darker so that the distinction survives in black and white. The strong El Niño episodes of 1997–98, 2015–16 and 2023–24 and the strong La Niña episodes of 1998–2000, 2010–11 and 2020–22 are the events that identify the results. The predictive regressions use this series centered at $t-2$, the value published within month t.

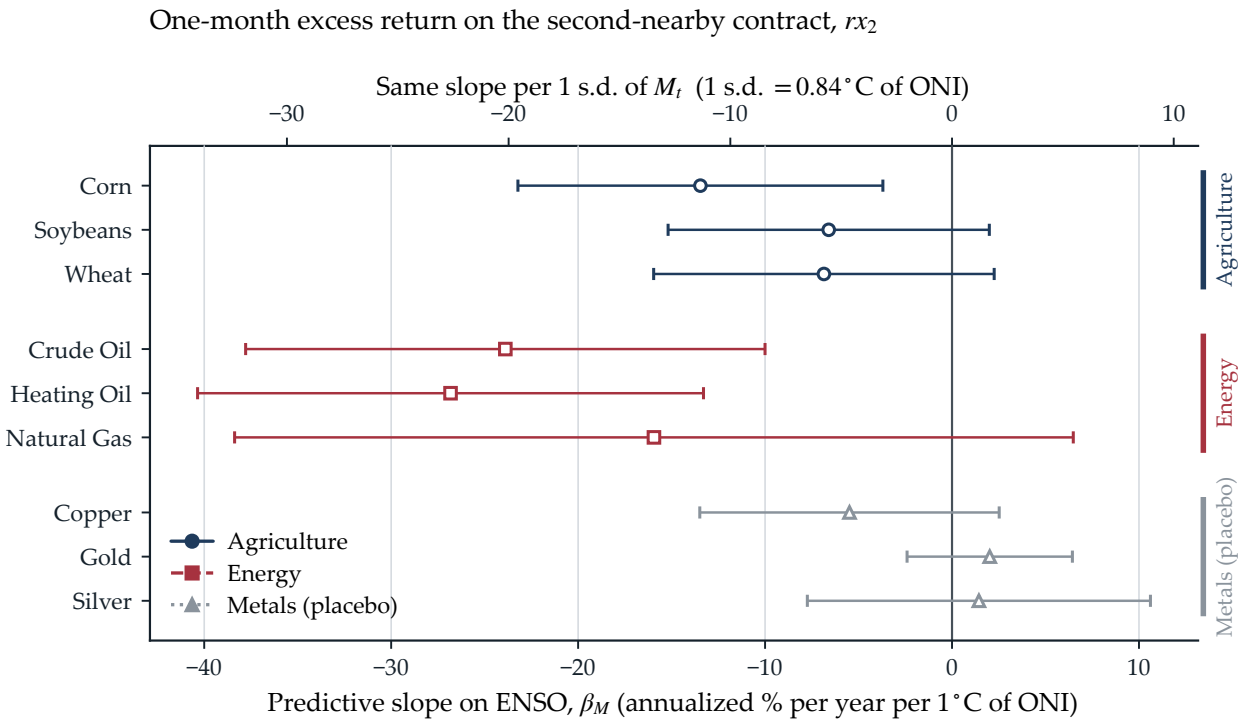


Figure 2: The ENSO slope by commodity. Point estimates of β_M from equation (3) on the second nearby contract, with 95% Newey–West confidence intervals (12 lags). The bottom axis is annualized percent per year per 1°C of ONI; the top axis rescales the same estimates to one standard deviation of the ENSO state (0.84°C). Markers are colored by sector: navy for agriculture, red for energy, gray for the metals placebo. All six weather-sensitive commodities lie on the negative side; gold and silver are positive.

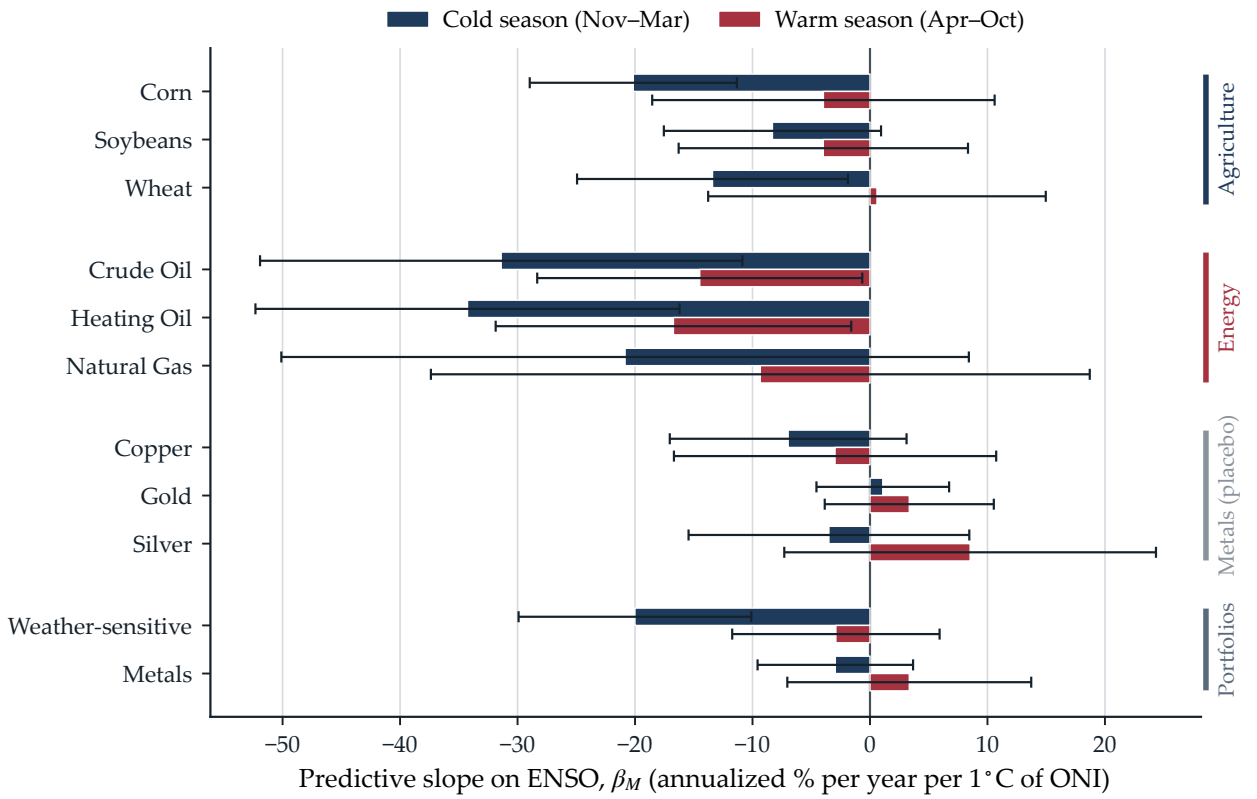


Figure 3: Cold-season and warm-season ENSO slopes. β_M^c (navy, cold season, November–March return months) and β_M^w (red, warm season) from the commodity-level regressions of Appendix Table A4, in annualized percent per year per 1°C of ONI, with 95% Newey–West confidence intervals (12 lags). The last two rows are the equal-weighted weather-sensitive and metals portfolios. The slope is more negative in the cold season for every weather-sensitive commodity, which is when the Pacific teleconnection over the Americas is strongest.

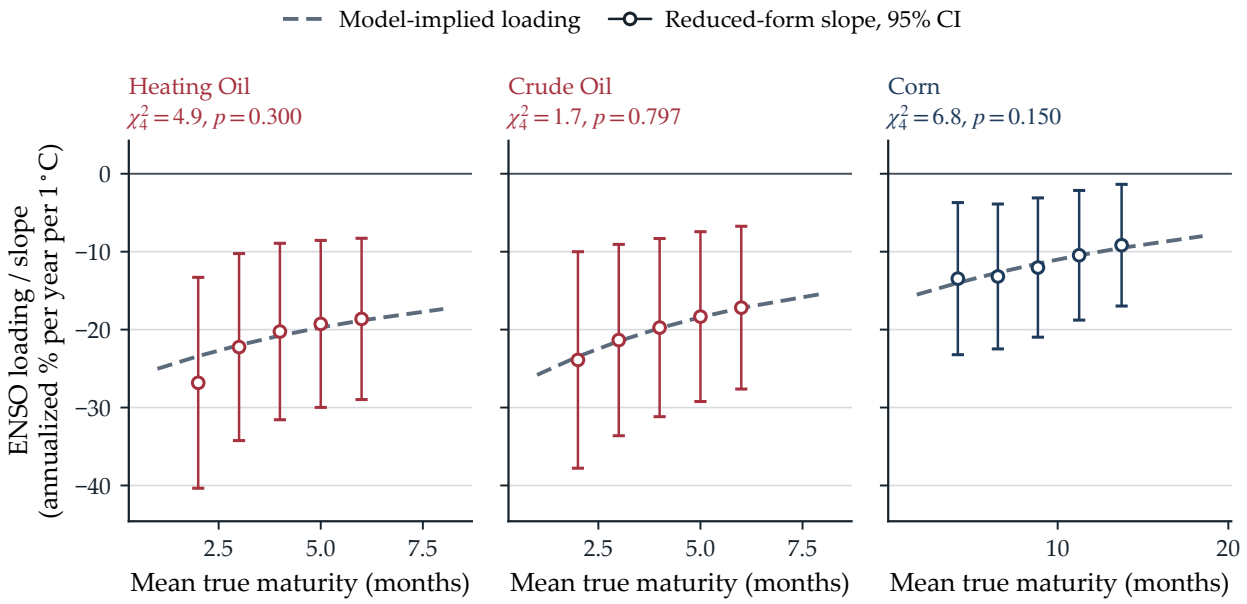


Figure 4: The model's maturity profile against freely estimated reduced-form slopes. Dark points with 95% Newey–West confidence intervals: ENSO slopes estimated separately for $rx_2, \ldots, rx_6$ from the same regressors, each placed at that contract's mean true months to expiry. Gray line: the model-implied ENSO loading $\boldsymbol{B}'_{\tau-1} K^{\mathbb{P}}_{1,LM}$, time-averaged over the realized maturity path of each contract. Units are annualized percent per year per 1°C of ONI. The three panels are heating oil, crude oil and corn. The reduced form does not impose the shape; the model predicts it from $K^{\mathbb{Q}}_1$, and the χ^2 shape test in each panel heading does not reject for any of the nine commodities.

Hedging pressure by ENSO phase, 1995-01–2026-02 (note the independent vertical scales)

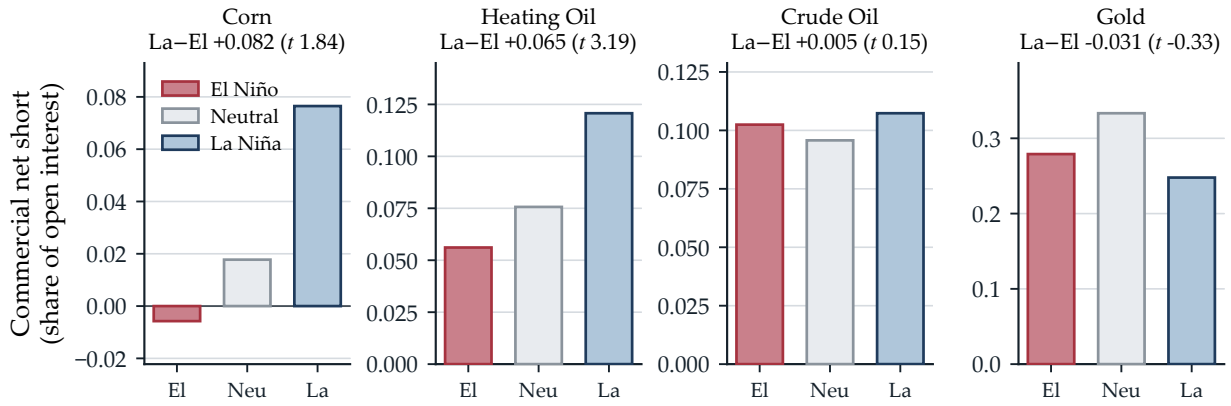


Figure 5: Hedging pressure by ENSO phase. Mean commercial net short position as a share of open interest, from the CFTC legacy futures-only Commitments of Traders reports, in El Niño months (red), neutral months (gray) and La Niña months (navy), for corn, heating oil, crude oil and the gold placebo. Each commodity has its own vertical scale, because the levels differ by an order of magnitude (gold's mean hedging pressure is 0.29 against corn's 0.03). The within-commodity phase gaps, annotated above each panel with their t-statistics, are the content of the figure. Producers hedge more heavily in La Niña, which is the state in which Table 6 shows realized returns are highest; gold shows no such pattern, and crude oil's gap is close to zero.

Appendix A Risk Premium Derivation

The one-period excess return on a contract with τ months to expiry at t is

$$rx_{t+1}^{(\tau)} = f_{t+1}^{(\tau-1)} - f_t^{(\tau)} = \left(A_{\tau-1} + \boldsymbol{B}_{\tau-1}' L_{t+1}\right) - \left(A_\tau + \boldsymbol{B}_\tau' L_t\right) + \left(\eta_{t+1}^{(\tau-1)} - \eta_t^{(\tau)}\right).$$

Ignoring measurement error and taking expectations under $\mathbb{P}$ using (5),

$$\mathbb{E}_t^{\mathbb{P}}\left[rx_{t+1}^{(\tau)}\right] = A_{\tau-1} - A_\tau + \boldsymbol{B}_{\tau-1}'\left(K_{0,L}^{\mathbb{P}} + K_{1,LL}^{\mathbb{P}} L_t + K_{1,LM}^{\mathbb{P}} M_t\right) - \boldsymbol{B}_\tau' L_t.$$

The Riccati recursions (11)–(12) give

$$A_{\tau-1} - A_\tau = -\boldsymbol{B}_{\tau-1}' K_0^{\mathbb{Q}} - \tfrac{1}{2}\boldsymbol{B}_{\tau-1}'\Omega_L \boldsymbol{B}_{\tau-1}, \qquad \boldsymbol{B}_\tau' L_t = \boldsymbol{B}_{\tau-1}' K_1^{\mathbb{Q}} L_t,$$

and substituting yields equation (13):

$$\begin{aligned}\mathbb{E}_t^{\mathbb{P}}\left[rx_{t+1}^{(\tau)}\right] = {} & \boldsymbol{B}_{\tau-1}'\left(K_{0,L}^{\mathbb{P}} - K_0^{\mathbb{Q}}\right) - \tfrac{1}{2}\boldsymbol{B}_{\tau-1}'\Omega_L \boldsymbol{B}_{\tau-1} \\ & + \boldsymbol{B}_{\tau-1}'\left(K_{1,LL}^{\mathbb{P}} - K_1^{\mathbb{Q}}\right) L_t + \boldsymbol{B}_{\tau-1}' K_{1,LM}^{\mathbb{P}} M_t. \qquad \square\end{aligned}$$

The market price of ENSO risk follows from the last block of (8): the unspanned restriction sets the ENSO column of the $\mathbb{Q}$-transition to zero, $\mathbf{0} = K_{1,LM}^{\mathbb{P}} - \Sigma_L \Lambda_{1,M}$, so $\Lambda_{1,M} = \Sigma_L^{-1} K_{1,LM}^{\mathbb{P}}$ with Σ_L the Cholesky factor of Ω_L.

Appendix B Estimation Details

We parametrize $K_1^{\mathbb{Q}}$ by setting $\det K_1^{\mathbb{Q}} = \tanh(a)$ and $\operatorname{tr} K_1^{\mathbb{Q}} = (1 + \det K_1^{\mathbb{Q}})\tanh(b)$, which traces out exactly the Schur stability triangle $\{|\det| < 1,\ |\operatorname{tr}| < 1 + \det\}$, the set of real 2×2 matrices with spectral radius below one; a rotation and a shear span the similarity class. Stationarity under $\mathbb{Q}$ therefore holds by construction and not by penalty, and the

parametrization reaches complex-conjugate eigenvalue pairs, though no estimate here has one. We use 24 seeded starting values, screen them with L-BFGS-B, polish the best five with Nelder–Mead followed by L-BFGS-B, and keep the best. For corn, copper and silver the spectral radius is at the boundary; for the other six it is slack (between 0.964 and 0.999). Across all starts within 0.5 log-likelihood units of the best, the ENSO loading does not move to the precision printed in Table 7 and the variance share moves by at most 0.6 percentage points; where only one start falls in that window the reported range is a point by construction.

The two curve factors enter (10) as observed regressors while the same seven prices are fitted with an i.i.d. error of standard deviation σ_η, so no portfolio of contracts is priced without error. This is not the Joslin et al. (2011) normalization, in which a set of portfolios is priced exactly; it is harmless for the loadings, but the RMSEs in Table A1 measure the fit of an over-identified system and are not directly comparable with JSZ-normalized numbers.

The Riccati recursions are run monthly to the longest maturity that occurs in the data (20 months for corn and wheat, 14 for soybeans and silver, 13 for gold, and 8 for the four chains that list every calendar month), and only observed contract-months enter the likelihood. The physical VAR (4) is estimated on calendar-consecutive month pairs only, so a missing month breaks the pair rather than creating a two-month "one-month" transition.

In the appendix variant of Table A9 a deterministic delivery-month effect γ is estimated outside the pricing model, by regressing log prices on observation-month fixed effects, delivery-month dummies and a quadratic in τ, and is subtracted before the principal components are extracted. The maturity control matters: without it the delivery month is, conditional on the observation month, a deterministic function of τ, and the cost of carry loads onto γ. The pricing model that follows has exactly the same parameter count as the baseline, so any change in fit is a change in the data being priced.

Appendix C Additional Tables and Figures

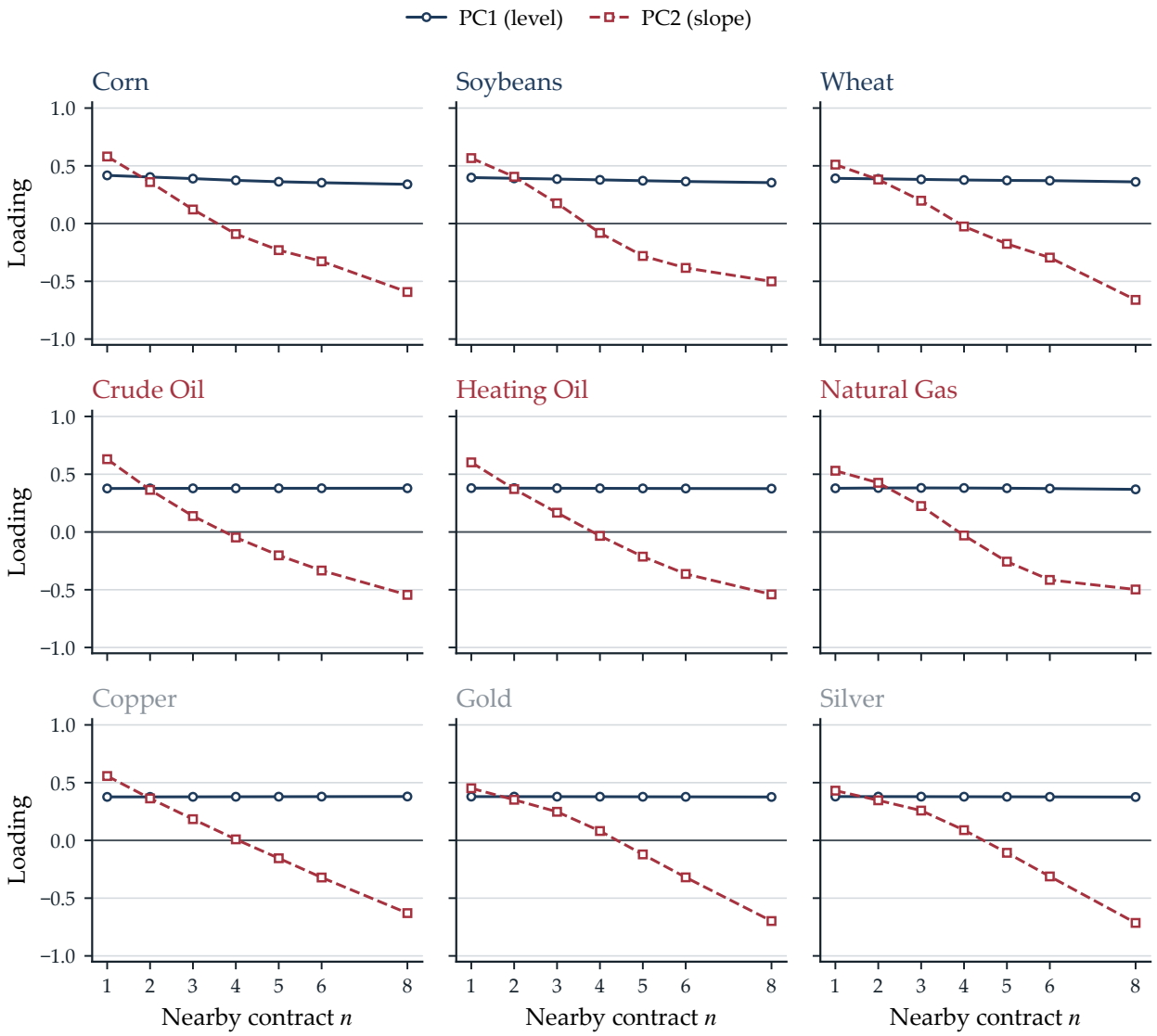


Figure A1: Principal component loadings. Loadings of the first two principal components of the log futures curve on each of the seven generic contracts, by commodity; navy for PC^1 (level), red for PC^2 (slope). Signs are normalized so that PC^1 up means prices up and PC^2 up means backwardation, which makes the sign of the ENSO slope comparable across commodities.

Table A1: The estimated affine model

Panel A: root mean squared pricing errors in percent of the log futures price, by generic contract; "Unrestr." lets every contract have free loadings and "$\tau = n$" re-estimates under the assumption that the n-th nearby has n months to expiry. **Panel B**: maximum-likelihood estimates of $K_1^{\mathbb{Q}}$, its eigenvalue moduli, the measurement-error standard deviation, the log-likelihood and the number of the 24 starts within 0.5 log-likelihood of the best. **Panel C**: the physical cross-block $K_{1,LM}^{\mathbb{P}}$, the implied market price of ENSO risk $\Lambda_{1,M} = \Sigma_L^{-1} K_{1,LM}^{\mathbb{P}}$, and the autoregressive coefficient of the ENSO state.

Panel A: pricing errors

Commodity	Sector	c_1	c_2	c_3	c_4	c_5	c_6	c_8	Avg.	Unrestr.	$\tau = n$
Corn	Agri.	1.93	1.73	2.38	2.30	2.22	2.25	2.20	2.14	2.00	2.01
Soybeans	Agri.	1.59	1.28	1.94	1.89	1.52	1.15	1.86	1.60	1.30	1.35
Wheat	Agri.	1.68	1.47	1.62	1.93	1.70	1.68	1.98	1.72	1.50	1.56
Crude Oil	Energy	0.69	0.30	0.48	0.45	0.26	0.13	0.63	0.42	0.42	0.42
Heating Oil	Energy	2.01	0.85	1.36	1.45	1.13	0.70	2.14	1.38	1.37	1.38
Natural Gas	Energy	5.13	2.41	4.08	5.01	4.46	3.55	7.04	4.53	4.37	4.53
Copper	Metals	0.36	0.17	0.24	0.25	0.19	0.09	0.31	0.23	0.23	0.23
Gold	Metals	0.09	0.04	0.06	0.09	0.11	0.13	0.19	0.10	0.07	0.11
Silver	Metals	0.18	0.10	0.17	0.14	0.16	0.18	0.26	0.17	0.15	0.19

Panel B: risk-neutral dynamics

Commodity	K_{11}^Q	K_{12}^Q	K_{21}^Q	K_{22}^Q	$\lvert\lambda_1\rvert$	$\lvert\lambda_2\rvert$	Cplx.	σ_η (%)	Log-lik.	Near-best
Corn	0.987	−0.188	−0.003	0.962	0.9999	0.9490	no	2.153	6858	5/24
Soybeans	0.990	−0.258	−0.000	0.899	0.9915	0.8982	no	1.630	8214	5/24
Wheat	0.995	−0.180	0.000	0.994	0.9948	0.9948	no	1.728	6499	1/24
Crude Oil	1.001	−0.437	0.001	0.840	0.9992	0.8413	no	0.460	12065	2/24
Heating Oil	0.998	−0.438	−0.000	0.861	0.9983	0.8613	no	1.466	8537	5/24
Natural Gas	0.996	−0.432	0.007	0.875	0.9639	0.9068	no	4.720	4942	4/24
Copper	1.001	−0.445	0.000	0.965	1.0000	0.9662	no	0.245	13985	2/24
Gold	0.999	−0.264	0.000	0.985	0.9979	0.9865	no	0.111	16396	3/24
Silver	0.999	−0.258	−0.000	0.998	1.0000	0.9973	no	0.177	14977	3/24

Panel C: the ENSO block and the price of ENSO risk

Commodity	$K_{1,LM}^P$ (PC1)	$K_{1,LM}^P$ (PC2)	$\Lambda_{1,M}$ (PC1)	$\Lambda_{1,M}$ (PC2)	$K_{1,MM}^P$
Corn	−0.0251	−0.0035	−0.15	−0.02	0.977
Soybeans	−0.0141	−0.0016	−0.09	−0.03	0.975
Wheat	−0.0170	−0.0007	−0.09	0.04	0.969
Crude Oil	−0.0413	−0.0063	−0.19	−0.04	0.980
Heating Oil	−0.0440	−0.0045	−0.20	−0.01	0.977
Natural Gas	−0.0225	−0.0038	−0.08	0.01	0.972
Copper	−0.0109	−0.0002	−0.06	0.01	0.974
Gold	0.0042	0.0000	0.04	0.01	0.973
Silver	0.0028	0.0001	0.01	0.02	0.971

Table A2: The ENSO loading across maturities, conventions and tests

Panel A: the model-implied ENSO loading $\boldsymbol{B}'_{\tau-1}K^{\mathbb{P}}_{1,LM}$ at true maturities $\tau = 2, \ldots, 8$, in percent per year per 1°C of ONI. The copper and silver rows are flat because both eigenvalues of their $K^{\mathbb{Q}}_1$ sit at or near one; corn's spectral radius is also at the boundary, but only through its level eigenvalue, so its profile still decays. **Panel B**: the $\tau = 2$ loading, the average pricing error and the log-likelihood under the true-maturity and $\tau = n$ conventions; the two coincide by construction for the chains that list every calendar month. Panel B is the one place loadings are printed to two decimals, because its content is that the two conventions agree to within 0.23. **Panel C**: Wald tests of the model's maturity profile against ENSO slopes estimated freely for $rx_2, \ldots, rx_6$ with a joint Newey–West covariance: a level test on all five and a shape test on the four slopes relative to rx_2, the latter being the informative one.

Panel A: term structure of the loading

Commodity	Sector	$\tau = 2$	$\tau = 3$	$\tau = 4$	$\tau = 5$	$\tau = 6$	$\tau = 7$	$\tau = 8$
Corn	Agri.	−15.3	−14.7	−14.1	−13.5	−12.9	−12.4	−11.9
Soybeans	Agri.	−8.0	−7.6	−7.2	−6.9	−6.6	−6.3	−6.1
Wheat	Agri.	−8.5	−8.4	−8.3	−8.2	−8.1	−8.0	−7.9
Crude Oil	Energy	−23.5	−21.5	−19.8	−18.4	−17.2	−16.2	−15.4
Heating Oil	Energy	−23.4	−22.0	−20.8	−19.7	−18.8	−18.0	−17.4
Natural Gas	Energy	−12.9	−11.9	−11.0	−10.1	−9.4	−8.7	−8.0
Copper	Metals	−5.1	−5.0	−5.0	−5.0	−4.9	−4.9	−4.9
Gold	Metals	2.0	1.9	1.9	1.9	1.9	1.9	1.9
Silver	Metals	1.3	1.3	1.3	1.3	1.3	1.3	1.2

Panel B: true maturities versus $\tau = n$

	ENSO loading, $\tau = 2$		Avg. RMSE (%)		Log-likelihood	
Commodity	True τ	$\tau = n$	True τ	$\tau = n$	True τ	$\tau = n$
Corn	−15.34	−15.11	2.143	2.014	6858	7024
Soybeans	−7.99	−7.95	1.604	1.346	8214	8706
Wheat	−8.46	−8.43	1.724	1.562	6499	6724
Crude Oil	−23.46	−23.46	0.420	0.420	12065	12065
Heating Oil	−23.40	−23.40	1.376	1.376	8537	8537
Natural Gas	−12.90	−12.90	4.527	4.527	4942	4942
Copper	−5.06	−5.06	0.230	0.230	13985	13985
Gold	1.95	1.96	0.102	0.107	16396	16352
Silver	1.34	1.35	0.171	0.189	14977	14683

Panel C: over-identification tests

	Shape test (rx_n vs rx_2)		Level test		
Commodity	χ^2_4	p	χ^2_5	p	Max |diff| in s.e.
Corn	6.75	0.150	6.84	0.233	0.11
Soybeans	3.96	0.412	4.09	0.537	0.22
Wheat	3.68	0.451	4.02	0.546	0.59
Crude Oil	1.67	0.797	1.74	0.883	0.06
Heating Oil	4.88	0.300	4.89	0.429	0.50
Natural Gas	4.16	0.385	4.53	0.475	0.31
Copper	4.94	0.294	4.94	0.423	0.10
Gold	0.65	0.957	0.71	0.983	0.03
Silver	3.40	0.493	3.54	0.618	0.04

Table A3: Spanning in detail, and the unspanned residual

Panel A: the R^2 of M_t projected on the curve factors, split by factor (each PC alone) and estimated separately within El Niño, neutral and La Niña months. The within-phase comparison is confounded by range restriction in M_t and is read as a direction, not a test. **Panel B**: the second step of the Jacobs et al. (2017) test, $\Delta PC^i_{t+1} = \alpha_i + \boldsymbol{\beta}'_{pc,i} L_t + \beta_{um,i} UM_t + \varepsilon_{i,t+1}$, where UM_t is the residual from that projection; coefficients are in principal-component units, Newey–West t-statistics with 12 lags.

Panel A: spanning by factor and by ENSO phase

	R^2 of M_t on the curve			By ENSO phase		
Commodity	Both PCs	PC^1 only	PC^2 only	El Niño	Neutral	La Niña
Corn	0.048	0.031	0.016	0.014	0.061	0.001
Soybeans	0.023	0.022	0.001	0.035	0.061	0.004
Wheat	0.024	0.020	0.004	0.027	0.024	0.006
Crude Oil	0.085	0.031	0.055	0.030	0.058	0.013
Heating Oil	0.056	0.025	0.031	0.034	0.059	0.025
Natural Gas	0.075	0.067	0.009	0.080	0.029	0.004
Copper	0.017	0.016	0.000	0.142	0.065	0.065
Gold	0.004	0.004	0.000	0.005	0.072	0.073
Silver	0.026	0.022	0.004	0.053	0.073	0.121

Panel B: the unspanned residual and future curve movements

		ΔPC^1_{t+1}			ΔPC^2_{t+1}		
Commodity	Sector	β_{um}	t	ΔR^2	β_{um}	t	ΔR^2
Corn	Agri.	−0.025	−2.61	0.016	−0.004	−2.08	0.006
Soybeans	Agri.	−0.014	−1.54	0.006	−0.002	−1.24	0.002
Wheat	Agri.	−0.017	−1.90	0.006	−0.001	−0.28	0.000
Crude Oil	Energy	−0.041	−3.32	0.022	−0.006	−2.50	0.014
Heating Oil	Energy	−0.044	−3.62	0.026	−0.005	−1.88	0.006
Natural Gas	Energy	−0.022	−1.25	0.004	−0.004	−0.65	0.001
Copper	Metals	−0.011	−1.27	0.003	−0.000	−0.36	0.000
Gold	Metals	0.004	0.85	0.001	0.000	0.21	0.000
Silver	Metals	0.003	0.28	0.000	0.000	0.32	0.000

Table A4: Cold versus warm season, commodity by commodity

β_M^c and β_M^w from $rx_{2,t+1} = \alpha + \boldsymbol{\beta}_{pc}' L_t + \beta_M^c(M_t \times \text{cold}_{t+1}) + \beta_M^w(M_t \times \text{warm}_{t+1}) + \varepsilon_{t+1}$, with cold meaning the return month falls in November–March; the last pair of columns tests equality. Newey–West t-statistics (12 lags); all estimates percent per year per 1°C of ONI. The cold-season slope is larger in absolute value for each of the six weather-sensitive commodities; among individual commodities the equality test rejects at 5% for corn alone.

	Cold season (Nov–Mar)		Warm season (Apr–Oct)		Difference	
Commodity / portfolio	β_M^c	t	β_M^w	t	$\beta^c - \beta^w$	t
Corn	−20.1	−4.48	−4.0	−0.53	−16.2	−2.18
Soybeans	−8.3	−1.76	−4.0	−0.63	−4.3	−0.64
Wheat	−13.4	−2.28	0.6	0.08	−14.0	−1.48
Crude Oil	−31.4	−3.00	−14.5	−2.05	−16.9	−1.46
Heating Oil	−34.3	−3.72	−16.7	−2.17	−17.5	−1.67
Natural Gas	−20.8	−1.40	−9.3	−0.65	−11.5	−0.61
Copper	−7.0	−1.35	−3.0	−0.42	−4.0	−0.45
Gold	1.1	0.38	3.3	0.91	−2.3	−0.47
Silver	−3.5	−0.57	8.5	1.06	−12.0	−1.09
Agriculture	−14.8	−3.50	−1.2	−0.20	−13.6	−2.35
Energy	−28.8	−3.32	−12.5	−1.59	−16.3	−1.64
Energy ex. nat. gas	−32.5	−3.46	−15.0	−2.15	−17.5	−1.66
Weather-sensitive	−20.0	−3.96	−2.9	−0.64	−17.1	−3.17
Metals	−3.0	−0.87	3.3	0.63	−6.3	−0.92
Weather-sens. − metals	−15.6	−2.24	−12.6	−1.77	−3.0	−0.36

Table A5: Robustness

Panel A: equation (3) on the second nearby, full sample and the two halves split at January 2008; columns are β_M and t for each. **Panel B**: the estimate and asymptotic t, then p-values from a circular moving-block bootstrap over months (24- and 36-month blocks, 4,999 draws) and from an episode-level t-test on q contiguous equal blocks in the spirit of Ibragimov and Müller (2010). **Panel C**: β_M with the ONI centered at t, $t-2$ (the baseline) and $t-3$; with the unconditional $c_n \to c_{n-1}$ return in place of the calendar-derived contract map; and re-estimated on last-trade instead of settlement prices. **Panel D**: the Driscoll–Kraay panel with the three ICE softs added, sector-specific slopes in that twelve-commodity panel, and the softs' own rx_2 regressions with their sample lengths. All slopes are percent per year per 1°C of ONI; t-statistics are Newey–West (12 lags) or Driscoll–Kraay as appropriate.

Row	(1)	(2)	(3)	(4)	(5)	(6)
Panel A: subsamples, rx_2 on M_t (full sample / through 2007 / from 2008)						
unit	β_M	t	β_M	t	β_M	t
Corn	−13.5	−2.70	−8.0	−1.33	−25.8	−3.16
Crude Oil	−23.9	−3.37	−23.1	−2.93	−29.6	−2.56
Heating Oil	−26.8	−3.89	−27.5	−2.54	−30.7	−3.47
Natural Gas	−15.9	−1.39	−4.2	−0.26	−34.6	−2.56
Gold	2.0	0.89	−4.9	−1.83	6.4	2.19
Agriculture	−8.7	−2.06	−1.7	−0.26	−21.3	−3.11
Energy ex. nat. gas	−25.1	−3.74	−25.4	−2.81	−29.6	−3.07
Weather-sensitive	−12.2	−3.01	−3.5	−0.51	−21.9	−3.40
Metals	−0.4	−0.14	−3.7	−1.16	0.6	0.12
Panel B: alternative inference (block bootstrap and ENSO-episode blocks)						
quantity	*est.*	*asy. t*	*boot p 24m*	*boot p 36m*	*episode p, $q=8$*	*$q=12$*
Panel: weather-sensitive	−15.8	−3.72	0.005	0.007	0.066	0.043
Panel: WS − metals	−15.1	−3.25	0.012	0.016	0.737	0.271
Panel: metals	−0.7	−0.23	0.817	0.797	0.106	0.030
Crude oil rx_2	−23.9	−3.37	0.005	0.004	0.088	0.083
Heating oil rx_2	−26.8	−3.89	0.000	0.001	0.003	0.058
Corn rx_2	−13.5	−2.70	0.032	0.041	0.029	0.051
Energy ex-nat. gas portfolio rx_2	−25.1	−3.74	0.003	0.002	0.021	0.075
Weather-sensitive portfolio rx_2	−12.2	−3.01	0.020	0.018	0.150	0.214
Seasonality: cold − warm	−13.7	−2.29	0.015	0.015	0.069	0.028
Panel C: ENSO timing, return definition and price source (β_M on rx_2)						
commodity	*ONI lag 0*	*lag 2 (base)*	*lag 3*	*no roll adj.*	*last trade*	*t*
Corn	−13.2	−13.5	−10.9	−13.5	−14.4	−2.82
Crude Oil	−25.1	−23.9	−22.5	−23.9	−23.6	−3.39
Heating Oil	−27.9	−26.8	−26.4	−26.8	−25.8	−3.88
Natural Gas	−18.5	−15.9	−14.9	−15.9	−15.8	−1.38
Soybeans	−7.4	−6.6	−4.6	−6.4	−6.4	−1.47
Wheat	−9.5	−6.9	−3.2	−3.7	−8.0	−1.53
Panel D: twelve commodities, adding cotton, coffee and sugar						
row	*β_M*	*t*	*p*	*obs.*	*months*	
Nine commodities: WS − metals	−15.1	−3.25	0.001	3,784	434	
Twelve commodities: WS − metals	−11.6	−2.94	0.003	4,818	434	
Twelve-commodity sector slope: Agriculture	−9.0	−2.21	0.027			
Twelve-commodity sector slope: Energy	−22.2	−3.21	0.001			
Twelve-commodity sector slope: Softs	−4.1	−0.79	0.428			
Twelve-commodity sector slope: Metals	−0.7	−0.23	0.815			
Cotton, rx_2	−2.0	−0.37		426		
Coffee, rx_2	−6.3	−0.89		323		
Sugar, rx_2	−4.8	−0.48		285		

Table A6: Subsample stability, all units

Equation (3) on the second nearby contract, estimated over the full sample and over the two halves split at January 2008; β_M is percent per year per 1°C of ONI with Newey–West t-statistics (12 lags) and T is the number of months. Table A5, Panel A reports a subset of these rows. Fourteen of the fifteen units have a larger slope in absolute value in the second half; energy excluding natural gas is the only group significant at 5% in both halves.

	Full sample			Through 2007-12			2008-01–2026-02		
Commodity / portfolio	β_M	t	T	β_M	t	T	β_M	t	T
Corn	−13.5	−2.70	400	−8.0	−1.33	182	−25.8	−3.16	218
Soybeans	−6.6	−1.50	434	−1.2	−0.22	216	−19.2	−2.42	218
Wheat	−6.9	−1.47	349	−2.9	−0.45	131	−25.1	−3.24	218
Crude Oil	−23.9	−3.37	434	−23.1	−2.93	216	−29.6	−2.56	218
Heating Oil	−26.8	−3.89	434	−27.5	−2.54	216	−30.7	−3.47	218
Natural Gas	−15.9	−1.39	431	−4.2	−0.26	213	−34.6	−2.56	218
Copper	−5.5	−1.34	434	−6.3	−0.92	216	−13.0	−1.81	218
Gold	2.0	0.89	434	−4.9	−1.83	216	6.4	2.19	218
Silver	1.4	0.31	434	−1.0	−0.18	216	1.4	0.16	218
Agriculture	−8.7	−2.06	348	−1.7	−0.26	130	−21.3	−3.11	218
Energy	−22.1	−3.23	431	−18.6	−1.69	213	−29.3	−3.37	218
Energy ex. nat. gas	−25.1	−3.74	434	−25.4	−2.81	216	−29.6	−3.07	218
Weather-sensitive	−12.2	−3.01	348	−3.5	−0.51	130	−21.9	−3.40	218
Metals	−0.4	−0.14	434	−3.7	−1.16	216	0.6	0.12	218
Weather-sens. − metals	−14.0	−2.53	348	5.4	0.54	130	−18.7	−3.06	218

Table A7: ENSO and the futures basis, commodity by commodity

Contemporaneous regressions of the basis on M_t. The basis is $(f_t^{(1)} - f_t^{(6)})$ divided by the actual number of months between the two expiries and annualized to percent; positive means backwardation. β_M^{con} is percent per year per 1°C of ONI, with Newey–West t-statistics (12 lags). $R^2_{b|L}$ is the R^2 of the basis on the commodity's own curve factors; because its median is 96%, the regressions include no curve controls. The panel version is Table 3, Panel C.

	Basis (%/yr)		Contemporaneous regression on M_t			
Commodity / portfolio	Mean	S.D.	β_M^{con}	t	R^2	$R^2_{b\|L}$
Corn	−5.0	10.5	−2.5	−1.73	0.042	0.961
Soybeans	1.3	10.7	−1.1	−0.99	0.007	0.965
Wheat	−8.1	8.7	0.4	0.32	0.002	0.945
Crude Oil	1.5	16.6	−4.5	−2.14	0.051	0.992
Heating Oil	1.5	20.0	−4.6	−1.91	0.038	0.943
Natural Gas	−13.2	40.7	−5.2	−1.42	0.012	0.916
Copper	1.0	7.1	0.2	0.20	0.000	0.983
Gold	−2.9	1.9	−0.0	−0.13	0.000	0.982
Silver	−3.2	2.1	−0.3	−0.84	0.011	0.957
Agriculture	−3.5	8.0	−0.9	−0.79	0.009	0.971
Energy	−3.4	21.1	−4.7	−2.19	0.036	0.905
Energy ex. nat. gas	1.5	16.6	−4.5	−2.10	0.053	0.971
Weather-sensitive	−3.6	11.6	−3.2	−2.22	0.052	0.825
Metals	−1.7	2.1	−0.0	−0.16	0.000	0.372

Table A8: Physical links: heating degree days and inventories

Panel A regresses the physical state on the ENSO state: the deseasonalized contiguous-U.S. heating-degree-day anomaly (NOAA/NCEI, Fahrenheit degree days, deseasonalized by full-sample calendar-month means), in degree days per 1°C of ONI; and the h-month change in EIA distillate stocks and natural gas storage, in percent per 1°C. **Panel B** regresses prices on the physical state: cold-season excess returns on the heating-degree-day anomaly per 100 degree days, and the basis and excess return on the inventory anomaly per one standard deviation. Each inventory series is lagged by its publication delay before use. Newey–West t-statistics (12 lags).

Link	Specification	β	t	R^2	T
Panel A: ENSO → the physical state (first leg)					
Heating degree days	Predictive, Cold (Nov–Mar)	−6.6	−1.20	0.008	181
Heating degree days	Contemporaneous, Deep winter (Dec–Feb)	−12.6	−2.34	0.029	109
Distillate stocks	Change over 1 month	0.30	0.74	0.002	220
Distillate stocks	Change over 3 months	0.88	0.88	0.005	220
Distillate stocks	Change over 6 months	1.43	1.17	0.009	220
Natural gas storage	Change over 1 month	0.21	1.56	0.004	255
Natural gas storage	Change over 3 months	0.58	1.26	0.003	255
Natural gas storage	Change over 6 months	0.69	0.95	0.002	253
Panel B: the physical state → prices (second leg)					
Heating Oil: HDD	rx_2, cold season	41.3	3.41	0.050	181
Natural Gas: HDD	rx_2, cold season	122.9	5.40	0.194	179
Heating Oil: inventory	Basis, per 1 s.d.	−10.2	−6.45	0.260	435
Heating Oil: inventory	rx_2, per 1 s.d.	−1.1	−0.23	0.000	434
Natural Gas: inventory	Basis, per 1 s.d.	−12.5	−5.16	0.094	432
Natural Gas: inventory	rx_2, per 1 s.d.	−3.6	−0.46	0.000	431

Table A9: The affine model with a deterministic delivery-month seasonal

The baseline model against a variant in which a deterministic delivery-month effect is estimated outside the pricing model and subtracted before the principal components are extracted (Appendix B). "γ range" is the peak-to-trough delivery-month effect in percent. Excess returns are numerically unchanged, because the roll-aware return holds the same contract from t to $t+1$ and the seasonal differences out; the ENSO loadings move only through the re-extracted factors.

	Avg. RMSE (%)		ENSO loading, $\tau = 2$		
Commodity	Baseline	Seasonal	Baseline	Seasonal	γ range (%)
Corn	2.143	1.838	−15.34	−14.95	3.3
Soybeans	1.604	1.288	−7.99	−7.75	3.3
Wheat	1.724	1.582	−8.46	−8.58	1.9
Crude Oil	0.420	0.432	−23.46	−23.35	0.5
Heating Oil	1.376	1.017	−23.40	−23.09	5.1
Natural Gas	4.527	2.735	−12.90	−14.97	17.3
Copper	0.230	0.232	−5.06	−5.06	0.1
Gold	0.102	0.103	1.95	1.95	0.1
Silver	0.171	0.171	1.34	1.33	0.1

Table A10: Settlement versus last-trade prices

Headline quantities re-estimated on the last-trade panel. Settlement is the baseline because it is the price at which the exchange marks positions and because it is more complete: switching adds between 0 and 44 months of usable returns per commodity, with the largest gains where the two fields disagree most.

	Settlement (baseline)		Last trade		Difference	
Headline	Est.	t	Est.	t	Δ est.	Δt
A3 rx2 Corn	−13.46	−2.70	−14.42	−2.82	0.96	0.12
A3 rx2 Soybeans	−6.60	−1.50	−6.45	−1.47	−0.15	−0.04
A3 rx2 Wheat	−6.85	−1.47	−7.97	−1.53	1.12	0.06
A3 rx2 Crude Oil	−23.89	−3.37	−23.57	−3.39	−0.33	0.02
A3 rx2 Heating Oil	−26.82	−3.89	−25.76	−3.88	−1.06	−0.00
A3 rx2 Natural Gas	−15.94	−1.39	−15.78	−1.38	−0.16	−0.01
A3 rx2 Copper	−5.48	−1.34	−5.39	−1.34	−0.10	0.00
A3 rx2 Gold	2.02	0.89	2.87	1.27	−0.86	−0.38
A3 rx2 Silver	1.44	0.31	−2.77	−0.53	4.21	0.84
A4 panel: weather-sensitive	−15.79	−3.72	−15.97	−3.73	0.18	0.01
A4 panel: WS - metals interaction	−15.11	−3.25	−14.25	−3.02	−0.87	−0.23
A4 panel: metals	−0.67	−0.23	−1.72	−0.60	1.05	0.37
A5b WS cold	−21.77	−4.08	−21.55	−3.89	−0.23	−0.19
A5b WS warm	−8.06	−1.66	−8.74	−1.77	0.68	0.11
A5b WS cold - warm	−13.71	−2.29	−12.81	−2.01	−0.90	−0.28
A12 energy ex-NG: El Nino - La Nina	−62.38	−3.98	−60.84	−4.05	−1.53	0.08
A8 loading (tau=2) Corn	−15.34	—	−16.61	—	1.28	—
A8 loading (tau=2) Soybeans	−7.99	—	−7.91	—	−0.08	—
A8 loading (tau=2) Wheat	−8.46	—	−9.65	—	1.19	—
A8 loading (tau=2) Crude Oil	−23.46	—	−23.48	—	0.02	—
A8 loading (tau=2) Heating Oil	−23.40	—	−22.81	—	−0.58	—
A8 loading (tau=2) Natural Gas	−12.90	—	−13.21	—	0.31	—
A8 loading (tau=2) Copper	−5.06	—	−4.85	—	−0.21	—
A8 loading (tau=2) Gold	1.95	—	2.07	—	−0.12	—
A8 loading (tau=2) Silver	1.34	—	−1.21	—	2.55	—

Table A11: Data diagnostics

Panel A: for each commodity and each calendar month of $t+1$, the standard deviation of $f_{t+1}^{(1)} - f_t^{(2)}$ (the return if the chain rolled) relative to that of $f_{t+1}^{(1)} - f_t^{(1)}$ (the return if it did not); a ratio below one indicates a roll. The separation is clear for the three grains, whose front contract does not turn over every month; for the six chains in which a contract expires every month the test cannot discriminate, which is why the contract calendar is validated against the exchange expiry field instead. **Panel B**: median monthly volume, the share of months with a price identical to the previous month, and the share with zero or missing volume, for the first and eighth nearby contracts of the last-trade panel.

Panel A: roll calendars

Commodity	Listing	Delivery months	Roll months	Mean ratio (roll)	Mean ratio (other)
Corn	cycle only	3, 5, 7, 9, 12	3, 5, 7, 9, 12	0.882	1.109
Soybeans	cycle only	1, 3, 5, 7, 8, 9, 11	1, 3, 5, 7, 8, 9, 11	0.956	1.043
Wheat	cycle only	3, 5, 7, 9, 12	3, 5, 7, 9, 12	0.944	1.071
Crude Oil	monthly	all	all	0.995	—
Heating Oil	monthly	all	all	0.991	—
Natural Gas	monthly	all	all	0.943	—
Copper	monthly	all	all	1.003	—
Gold	cycle + 3 serial	2, 4, 6, 8, 10, 12	all	0.996	—
Silver	cycle + 3 serial	1, 3, 5, 7, 9, 12	all	0.998	—

Panel B: price staleness and liquidity in the last-trade panel

	1st nearby			8th nearby		
Commodity	Median volume	Unchanged (%)	Zero vol. (%)	Median volume	Unchanged (%)	Zero vol. (%)
Corn	1,180,632	0.2	0.0	3,325	0.8	7.6
Soybeans	643,219	0.5	0.0	9,344	1.0	0.2
Wheat	484,180	0.0	0.0	725	1.3	23.0
Crude Oil	4,385,372	0.2	0.0	72,123	0.2	0.0
Heating Oil	620,228	0.5	0.0	16,416	0.2	0.0
Natural Gas	1,285,164	0.0	0.0	44,900	0.9	0.0
Copper	13,556	0.5	0.0	2,047	0.2	0.0
Gold	11,811	0.5	0.0	4,114	0.5	0.0
Silver	5,311	0.0	0.0	1,237	0.5	1.6